

A comparative analysis of results on B-anomalies using a machine learning algorithm

J. ALDA^{a,b,c1}, A. MIR^{c,d2}, S. PEÑARANDA^{c,d3}

^a*Dipartimento di Fisica ed Astronomia “Galileo Galilei”, Università degli Studi di Padova, via F. Marzolo 8, 35131 Padova, Italy*

^b*Istituto Nazionale di Fisica Nucleare (INFN), Sezione Padova, via F. Marzolo 8, 35131 Padova, Italy*

^c*Centro de Astropartículas y Física de Altas Energías (CAPA), Universidad de Zaragoza, Zaragoza, Spain*

^d*Departamento de Física Teórica, Facultad de Ciencias, Universidad de Zaragoza, Pedro Cerbuna 12, E-50009 Zaragoza, Spain*

Abstract

We present an analysis on flavour anomalies in semileptonic rare B -meson decays using an effective field theory approach and assuming that new physics affects only one generation in the interaction basis and non-universal mixing effects are generated by the rotation to the mass basis. A global fit to experimental data is performed, focusing on LFU ratios $R_{D^{(*)}}$ and $R_{J/\psi}$ and branching ratios that exhibit tensions with Standard Model predictions on $B \rightarrow K^{(*)}\nu\bar{\nu}$ decays. We use a Machine Learning Montecarlo algorithm in our analysis. Comparing three different scenarios, we show that the one that introduces only mixing between the second and third quark generations and no mixing in the lepton sector, as well as independent coefficients for the singlet and triplet four fermion effective operators, provides the best fit to experimental data. A comparison with previous results is performed.

¹jorge.alda@pd.infn.it

²amir@unizar.es

³siannah@unizar.es

1 Introduction

In the last decade several experimental anomalies related to flavour physics and, in particular, in B -meson decays, have been observed [1–18]. The disagreement between the theoretical predictions in the Standard Model (SM) and the experimental measurements is a clear open window for searches of physics beyond the SM. A model-independent analysis of the contributions to B -physics observables displaying those discrepancies is highly recommended. The Effective Field Theory (EFT) approach allows us to perform this kind of analysis by focusing on the relevant degrees of freedom and describing the physics one is interested in [19–22]. In this way, we can study the allowed regions of parameter space which are compatible with experimental results.

In order to better identify the possible deviations from the SM behaviour, one can construct ratios of branching ratios, which are “cleaner” observables as hadronic uncertainties largely cancel. For example, the $R_{D^{(*)}}$ ratios,

$$R_{D^{(*)}}^\ell = \frac{\text{BR}(B \rightarrow D^{(*)}\tau\bar{\nu}_\tau)}{[\text{BR}(B \rightarrow D^{(*)}e\bar{\nu}_e) + \text{BR}(B \rightarrow D^{(*)}\mu\bar{\nu}_\mu)]/2}, \quad (1)$$

whose values in the SM are [23]:

$$R_D^{SM} = 0.299 \pm 0.004, \quad R_{D^*}^{SM} = 0.257 \pm 0.005. \quad (2)$$

The latest measurements of the $R_{D^{(*)}}$ ratios have been performed at Belle II [16],

$$R_{D^*}^\ell = 0.262^{+0.041+0.035}_{-0.039-0.032}, \quad (3)$$

and LHCb [17],

$$\begin{aligned} R_D^\ell &= 0.249 \pm 0.043 \pm 0.047, \\ R_{D^*}^\ell &= 0.402 \pm 0.081 \pm 0.085, \end{aligned} \quad (4)$$

bringing the world average to [24]

$$\begin{aligned} R_D^\ell &= 0.342 \pm 0.026, \\ R_{D^*}^\ell &= 0.287 \pm 0.012, \end{aligned} \quad (5)$$

which are 1.6σ and 2.5σ above the SM, respectively, with a combined tension of 3.31σ .

Another class of B meson observables is $R_{J/\psi}$, defined as the Lepton Flavour Universality (LFU) ratio,

$$R_{J/\psi} = \frac{\text{BR}(B_c \rightarrow J/\psi\tau\bar{\nu}_\tau)}{\text{BR}(B_c \rightarrow J/\psi\mu\bar{\nu}_\mu)}. \quad (6)$$

At the quark level, it corresponds to a $b \rightarrow c\ell\nu$ transition, which is the same transition as the R_D and R_{D^*} ratios. As such, it is natural to examine the $R_{J/\psi}$ ratio looking for a similar anomaly. Indeed, the SM prediction is [25]

$$R_{J/\psi}^{SM} = 0.258 \pm 0.004, \quad (7)$$

while the experimental measurement at LHCb [26]

$$R_{J/\psi}^{\text{LHCb}} = 0.71 \pm 0.17 \pm 0.18, \quad (8)$$

displaying a 1.8σ tension. It is interesting to note that the experiments detect an excess of tauonic decays (or equivalently a defect of light lepton decays), which is also the case for the R_D and R_{D^*} anomalies. However, this tension is not present in the recent measurement at CMS [15]

$$R_{J/\psi}^{\text{CMS}} = 0.17^{+0.18+0.21+0.19}_{-0.17-0.22-0.18}, \quad (9)$$

which is only 0.3σ away from the SM prediction. The naïve average of both measurements results in [27]

$$R_{J/\psi} = 0.52 \pm 0.20, \quad (10)$$

consistent with the SM prediction at the 1.3σ level.

Besides, Belle II has also reported an excess in the $B^+ \rightarrow K^+\nu\bar{\nu}$ decay [28], combining inclusive and hadronic tagging,

$$\text{BR}(B^+ \rightarrow K^+\nu\bar{\nu}) = (2.3 \pm 0.7) \times 10^{-5}, \quad (11)$$

which present a 2.7σ excess as compared to the SM prediction [29],

$$\text{BR}(B^+ \rightarrow K^+\nu\bar{\nu})_{\text{SM}} = (0.429 \pm 0.013 \pm 0.02) \times 10^{-5}. \quad (12)$$

For the decay into a vector kaon, the 90% confidence level limit set by Belle [30],

$$\text{BR}(B^0 \rightarrow K^{*0}\nu\bar{\nu}) < 1.8 \times 10^{-5}, \quad \text{BR}(B^+ \rightarrow K^{*+}\nu\bar{\nu}) < 6.1 \times 10^{-5}, \quad (13)$$

is at least still a factor of 2 away from the SM prediction [31],

$$\text{BR}(B \rightarrow K^*\nu\bar{\nu})_{\text{SM}} = (0.824 \pm 0.099) \times 10^{-5}. \quad (14)$$

The experimental data has been used in recent years to constrain New Physics (NP) models. Several global fits have been performed in the literature [19–22, 24, 25, 27, 32–46], and references therein. The present work includes in the global analysis the recent experimental measurements of R_{D^*} [24] and $R_{J/\psi}$ [27], by improving several aspects of our previous article [19]. We discuss the implications of these recent measurements in our analysis. Besides, the latest results for $B^+ \rightarrow K^+\nu\bar{\nu}$ decay are also included in the discussion.

In this paper, the ratios of branching fractions for the $b \rightarrow s\ell^+\ell^-$ processes, R_K and R_{K^*} , which have been exhaustively studied in our previous works [19–22], will not be that important. That is because recent experimental data [47] has resolved the discrepancies that previously existed between experimental measurements and the SM predictions. As a result, these ratios no longer present the same level of interest for exploring potential deviations from the SM, and thus, our focus will shift to the previously shown observables where significant discrepancies remain. For completeness and comparison with our previous results [19], the present experimental measurements for the ratios R_K and R_{K^*} are included in the global fits.

The paper is organized as follows. Section 2 provides a summary of the relevant terms of the Weak Effective Theory for our analysis, as well as few details on how to perform the statistical fit of the Wilson coefficients involved. We analyse the $b \rightarrow c\tau\bar{\nu}$ and the $B \rightarrow K^{(*)}\nu\bar{\nu}$ decays, providing the best fit predictions for R_{D^*} and $R_{J/\psi}$ observables and for the $B^+ \rightarrow K^+\nu\bar{\nu}$ and $B^0 \rightarrow K^{*0}\nu\bar{\nu}$ branching ratios. Section 3 is devoted to the global fits, by including a detailed comparison with our previous results and a few details of the Machine Learning Montecarlo algorithm used up. At the end of this section we discuss the correlation for the R_{D^*} observable and $B^+ \rightarrow K^+\nu\bar{\nu}$ decay. Finally, conclusions are presented in section 4. Appendix A contains the list of observables that contribute to the global fit, by giving their prediction in the new scenario considered in this work.

2 Effective field theories

The Weak Effective Theory (WET) is formulated at an energy scale below the electroweak scale and the heavy SM states (t , h , W^\pm and Z^0) are integrated out. The NP resides at an energy that is greater than the experimentally accessible energies, and the Wilson coefficients are a measure of the strength with which the NP couples to ordinary particles. The dimension six operators are constructed from light SM fields. In this section we only present the relevant terms for our analysis from the WET Lagrangian [48–50]. We start by analyzing the $b \rightarrow c\tau\bar{\nu}$ decays and then discuss the $B \rightarrow K^{(*)}\nu\bar{\nu}$ decays. The best fit predictions for R_{D^*} and $R_{J/\psi}$ observables and for the $B^+ \rightarrow K^+\nu\bar{\nu}$ and $B^0 \rightarrow K^{*0}\nu\bar{\nu}$ branching ratios are obtained.

2.1 $b \rightarrow c\tau\bar{\nu}$ decays

In the WET below the electroweak scale, the expressions for $R_{J/\psi}$ were given by [25, 51], and for $R_{D^{(*)}}$ by [52]. The relevant effective Lagrangian is

$$\mathcal{L}_{b \rightarrow c\tau\nu} = -\frac{4G_F}{\sqrt{2}} V_{cb} [(1 + C_{VL}) O_{VL} + C_{VR} O_{VR} + C_{SL} O_{SL} + C_{SR} O_{SR} + C_T O_T] + \text{h.c.}, \quad (15)$$

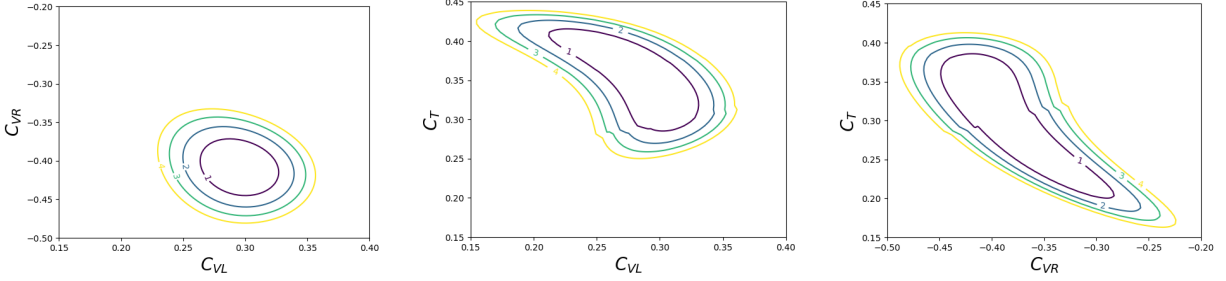


Figure 1: Fit to the WET parameters to the R_{D^*} and $R_{J/\psi}$ ratios at 1σ (purple), 2σ (blue), 3σ (green) and 4σ (yellow).

where G_F is the Fermi constant, V_{cb} is an element of the CKM matrix and the effective operators are defined as

$$\begin{aligned} O_{VL} &= (\bar{c}_L \gamma^\mu b_L)(\bar{\tau}_L \gamma_\mu \nu_L), & O_{VR} &= (\bar{c}_R \gamma^\mu b_R)(\bar{\tau}_L \gamma_\mu \nu_L), \\ O_{SL} &= (\bar{c}_R b_L)(\bar{\tau}_R \nu_L), & O_{SR} &= (\bar{c}_L b_R)(\bar{\tau}_R \nu_L), \\ O_T &= (\bar{c}_R \sigma^{\mu\nu} b_L)(\bar{\tau}_R \sigma_{\mu\nu} \nu_L), \end{aligned} \quad (16)$$

being their corresponding Wilson coefficients $C_{VL}, C_{VR}, C_{SL}, C_{SR}$ and C_T , respectively.

In the SM, the $b \rightarrow c l \nu$ transitions at tree level are mediated by the exchange of a W boson, which in the WET is integrated out contributing to the $C_{VL}^{\text{tot}} = 1 + C_{VL}$ Wilson coefficient. This contribution has already been separated in Lagrangian (15), and therefore any nonzero value of the Wilson coefficients in the Lagrangian will be due only to NP. The dominant contribution will come from the interference term between C_{VL} and the SM. Furthermore, the scalar contributions C_{SL} and C_{SR} are helicity-suppressed by the mass of the lepton [53].

The NP contributions at an energy scale $\Lambda \sim \mathcal{O}(\text{TeV})$ are defined via the Standard Model Effective Field Theory (SMEFT) Lagrangian [54]. The relevant terms for our analysis can be written as,

$$\mathcal{L}_{\text{SMEFT}} = \frac{1}{\Lambda^2} \left(C_{\ell q(1)}^{ijkl} O_{\ell q(1)}^{ijkl} + C_{\ell q(3)}^{ijkl} O_{\ell q(3)}^{ijkl} \right), \quad (17)$$

where ℓ and q are the lepton and quark $SU(2)_L$ doublets, i, j, k, l denote generation indices, Λ is the energy scale, the dimension six operators are defined as

$$O_{\ell q(1)}^{ijkl} = (\bar{\ell}_i \gamma_\mu \ell_j)(\bar{q}_k \gamma^\mu q_l), \quad O_{\ell q(3)}^{ijkl} = (\bar{\ell}_i \gamma_\mu \tau^I \ell_j)(\bar{q}_k \gamma^\mu \tau^I q_l), \quad (18)$$

with τ^I being the Pauli matrices and $C_{\ell q(1)}^{ijkl}$ and $C_{\ell q(3)}^{ijkl}$ are the corresponding Wilson coefficients. Here we only include the SMEFT operators containing two left-handed quarks and two left-handed leptons motivated by our interest in the B anomalies.

The tree-level matching between the WET and SMEFT coefficients at the scale $\mu = M_Z$ is given by [55]:

$$\begin{aligned} C_{VL} &= -\frac{\sqrt{2}}{4G_F \Lambda^2 V_{cb}} \left(2C_{\ell q(3)}^{3323} - 2C_{\varphi q(3)}^{23} \right), & C_{VR} &= \frac{\sqrt{2}}{4G_F \Lambda^2 V_{cb}} C_{\varphi ud}^{23} \\ C_{SL} &= -\frac{\sqrt{2}}{4G_F \Lambda^2 V_{cb}} C_{\ell equ(1)}^{3332*}, & C_{SR} &= -\frac{\sqrt{2}}{4G_F \Lambda^2 V_{cb}} C_{\ell edq}^{3332*}, \\ C_T &= -\frac{\sqrt{2}}{4G_F \Lambda^2 V_{cb}} C_{\ell equ(3)}^{3332*}. \end{aligned} \quad (19)$$

It is important to note that the contributions from scalar-quark operators $C_{\varphi q(3)}$ and $C_{\varphi ud}$ are universal in the lepton flavour, and therefore can not contribute to the B -meson anomalies. The contributions from $C_{\ell equ(1)}$, $C_{\ell equ(3)}$ and $C_{\ell edq}$ involve right-handed fermions, which are suppressed because they do not interfere with the SM electroweak interactions.

In order to better understand the impact of NP on $R_{J/\psi}$ and its relation to R_{D^*} , we perform a statistical fit of the three Wilson coefficients in C_{VR} , C_{VL} and C_T including both observables. As mentioned before, the contribution of the scalar coefficients are negligible. The fit is performed by numerical minimization of the statistic test χ^2 given by

$$\chi_{\text{fit}}^2 = \frac{1}{2} \sum_{i,j} [\mathcal{O}_i^{\text{exp}} - \mathcal{O}_i^{\text{th}}(\{C\})] \mathcal{C}_{ij}^{-1} [\mathcal{O}_j^{\text{exp}} - \mathcal{O}_j^{\text{th}}(\{C\})], \quad (20)$$

where $\mathcal{O}_i^{\text{exp}}$ and $\mathcal{O}_i^{\text{th}}(\{C\})$ are the experimental measurement and theoretical prediction for the i -th observable, respectively, and \mathcal{C}_{ij} is the correlation matrix. The result of the fit is represented in Figure 1, by choosing two-dimensional contours of the Wilson coefficients with the rest of the parameters as fixed in the best fit point. The scalar contributions C_{SL} and C_{SR} are suppressed and the fit is constrained by the vector Wilson coefficients C_{VL} and C_{VR} and the tensor coefficient C_T . The values obtained for each coefficient are:

$$C_{VL} = 0.296 \pm 0.167, \quad C_{VR} = -0.409 \pm 0.089, \quad C_T = 0.341 \pm 0.386. \quad (21)$$

The predictions for R_D , R_{D^*} and $R_{J/\psi}$ observables and their uncertainties in the best fit point are

$$R_D = 0.342^{+0.039}_{-0.039}, \quad R_{D^*} = 0.288^{+0.022}_{-0.022}, \quad R_{J/\psi} = 0.345^{+0.026}_{-0.029}, \quad (22)$$

compatible with the experimental results within 1σ .

2.2 $B \rightarrow K^{(*)}\nu\bar{\nu}$ decays

In the WET, the $B \rightarrow K^{(*)}\nu\bar{\nu}$ processes receive contributions from the effective operators appearing in the Lagrangian [29]

$$\mathcal{L}_{b \rightarrow s\nu\bar{\nu}} = -\frac{4G_F}{\sqrt{2}} \frac{\alpha_{\text{em}}}{4\pi} \sum_{\nu,\nu'} \left[(C_L^{\text{NP}\,\nu\nu'} + C_L^{\text{SM}\,\nu\nu'}) O_L^{\nu\nu'} + C_R^{\nu\nu'} O_R^{\nu\nu'} \right] + \text{h.c.}, \quad (23)$$

where the semileptonic four-fermion operators are

$$O_L^{\nu\nu'} = (\bar{s}\gamma_\mu P_L b)(\bar{\nu}\gamma^\mu P_L \nu'), \quad O_R^{\nu\nu'} = (\bar{s}\gamma_\mu P_R b)(\bar{\nu}\gamma^\mu P_R \nu'), \quad (24)$$

being $P_{R,L} = (1 \pm \gamma_5)/2$. The SM matching is $C_L^{\text{SM}\,\nu\nu'} = V_{tb} V_{ts}^* X_{\text{SM}} \delta_{\nu\nu'}$, where V_{ij} are the elements of the CKM matrix, and $X_{\text{SM}} = -12.64 \pm 0.15$ [29, 56]. The branching ratios in the WET are calculated as

$$\text{BR}(B^+ \rightarrow K^+\nu\bar{\nu}) = A_+^{BK} \sum_{\nu,\nu'} |(C_L^{\text{NP}\,\nu\nu'} + C_L^{\text{SM}\,\nu\nu'}) + C_R^{\nu\nu'}|^2, \quad (25)$$

$$\begin{aligned} \text{BR}(B^0 \rightarrow K^{*0}\nu\bar{\nu}) &= A_+^{BK*} \sum_{\nu,\nu'} |(C_L^{\text{NP}\,\nu\nu'} + C_L^{\text{SM}\,\nu\nu'}) + C_R^{\nu\nu'}|^2 \\ &+ A_-^{BK*} \sum_{\nu,\nu'} |(C_L^{\text{NP}\,\nu\nu'} + C_L^{\text{SM}\,\nu\nu'}) - C_R^{\nu\nu'}|^2, \end{aligned} \quad (26)$$

where $A_+^{BK} = (5.66 \pm 0.17) \times 10^{-6}$ [29] and $A_-^{BK*} = (8.88 \pm 1.08) \times 10^{-6}$, $A_+^{BK*} = (2.00 \pm 0.29) \times 10^{-6}$ [31].

The tree-level match between the relevant SMEFT and the WET Wilson coefficients is [55]

$$\begin{aligned} C_L^{\text{NP}\,\nu\nu'} &= -\frac{\sqrt{2}\pi}{G_F \Lambda^2 \alpha_{\text{em}}} \left(C_{\ell q(1)}^{\nu\nu'23} - C_{\ell q(3)}^{\nu\nu'23} + \delta_{\nu\nu'} C_{\varphi q(1)}^{23} + \delta_{\nu\nu'} C_{\varphi q(3)}^{23} \right), \\ C_R^{\nu\nu'} &= -\frac{\sqrt{2}\pi}{G_F \Lambda^2 \alpha_{\text{em}}} \left(C_{\ell d}^{\nu\nu'23} + \delta_{\nu\nu'} C_{\varphi d}^{23} \right). \end{aligned} \quad (27)$$

When performing a fit that considers only the parameters C_L^{33} and C_R^{33} (third generation of neutrinos), we observe that the resulting values are located at the intersection between two parallel

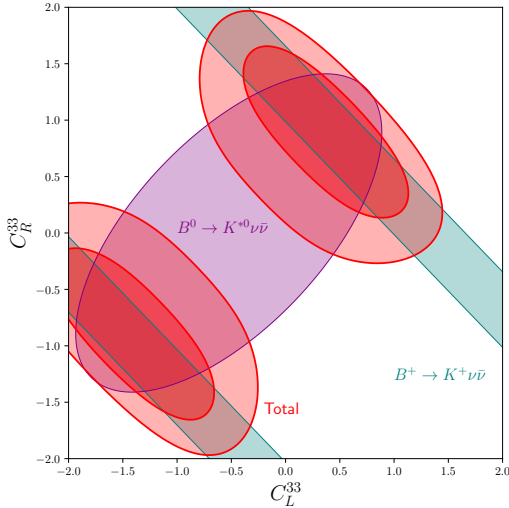


Figure 2: Fit to the WET parameters affecting the $B \rightarrow K^{(*)}\nu\bar{\nu}$ branching ratios. The teal areas correspond to $\text{BR}(B^+ \rightarrow K^+\nu\bar{\nu}) = (2.3 \pm 0.7) \times 10^{-5}$ and the purple area to $\text{BR}(B^0 \rightarrow K^{*0}\nu\bar{\nu}) < 1.8 \times 10^{-5}$, while the red areas are the best fit at 1σ and 2σ .

bands, which occur at $C_L^{33} + C_R^{33} = \text{constant}$, consequence of the constraints imposed by the observable $B^+ \rightarrow K^+\nu\bar{\nu}$; and the ellipse that corresponds to the constraints imposed by the observable $B^0 \rightarrow K^{*0}\nu\bar{\nu}$ as shown in Figure 2. The two minima are located at

$$(C_L^{33}, C_R^{33}) = (-1.4 \pm 0.6, -0.9 \pm 0.6) \quad \text{and} \quad (C_L^{33}, C_R^{33}) = (0.4 \pm 0.6, 0.9 \pm 0.6) \quad (28)$$

and in both minima the predictions for the observables are

$$\text{BR}(B^+ \rightarrow K^+\nu\bar{\nu}) = (2.2 \pm 0.7) \times 10^{-5}, \quad \text{BR}(B^0 \rightarrow K^{*0}\nu\bar{\nu}) = (1.3 \pm 0.2) \times 10^{-5}, \quad (29)$$

compatible with the experimental measurements. We reproduce the results of [29] for their cLFC scenario. If only couplings to left-handed quarks are allowed, the best fits are obtained for $C_L^{33} = 0.9 \pm 0.3$ or -2.0 ± 0.3 , corresponding to $\text{BR}(B^+ \rightarrow K^+\nu\bar{\nu}) = (1.5 \pm 0.6) \times 10^{-5}$ and $\text{BR}(B^0 \rightarrow K^{*0}\nu\bar{\nu}) = (1.8 \pm 1.0) \times 10^{-5}$. Therefore, we can conclude that C_L^{33} alone can reduce the tension to the 1σ level, while the addition of C_R^{33} is necessary to fully describe the experimental data.

3 Global fits

In this section we will update and extend the results obtained in [19], which used a subset of the SMEFT operators first proposed by [57–59]. The dimension-6 Lagrangian in the “Warsaw-down” basis takes the form [19]

$$\mathcal{L}_{\text{NP}} = \frac{\lambda_{ij}^\ell \lambda_{kl}^q}{\Lambda^2} [C_1(\bar{\ell}_i \gamma_\mu \ell_j)(\bar{q}_k \gamma^\mu q_\ell) + C_3(\bar{\ell}_i \gamma_\mu \tau^I \ell_j)(\bar{q}_k \gamma^\mu \tau^I q_\ell)], \quad (30)$$

where ℓ_i and q_i are the $SU(2)_L$ doublets for the i -th generation of leptons and quarks, respectively, Λ is the energy scale where the UV theory is matched to the SMEFT, C_1 and C_3 are the Wilson coefficients for singlet and triplet interactions, with the identification $C_{\ell q(1)}^{ijkl} = C_1 \lambda_{ij}^\ell \lambda_{kl}^q$ and $C_{\ell q(3)}^{ijkl} = C_3 \lambda_{ij}^\ell \lambda_{kl}^q$, being λ^ℓ and λ^q the matrices that determine the flavour structure of the NP interactions. We will fix the value $\Lambda = 1$ TeV, which assumes that the NP effects can be observed in flavour physics experiments. Flavour-changing charged currents can only be mediated by triplet interactions, and therefore C_3 is necessary to describe the $R_{D^{(*)}}$ and $R_{J/\psi}$ anomalies. Flavour-changing neutral currents, on the other hand, are mediated by both C_1 and C_3 , in particular the contributions to $b \rightarrow s\ell^+\ell^-$ are proportional to $C_1 + C_3$, while $b \rightarrow s\nu\bar{\nu}$ receives tree-level contributions from $C_1 - C_3$. Finally, the matrices λ are a reflection of the flavour structure of the UV theory. One simple case, proposed by [57], considered

	Scenario I	Scenario II	Scenario III
C_1	$-0.11^{+0.03}_{-0.04}$	-0.12 ± 0.03	-0.205 ± 0.015
C_3	$-0.11^{+0.03}_{-0.04}$	-0.12 ± 0.03	$-0.12^{+0.02}_{-0.01}$
α^ℓ	—	0.0 ± 0.07	—
β^ℓ	0.00 ± 0.02	0.000 ± 0.014	—
α^q	—	-0.076	—
β^q	$0.78^{+1.22}_{-0.36}$	$0.85^{+1.05}_{-0.6}$	$0.64^{+1.36}_{-0.24}$
Pull	5.71σ	5.51σ	6.25σ
$\Delta\chi^2_{\text{SM}}$	39.8	43.12	46.66
p -value	1.2×10^{-8}	3.5×10^{-8}	4.1×10^{-10}

Table 1: Results of the best fits to the rotation parameters and the coefficients C in Scenario I, II and III.

that the UV theory only affected one generation of fermions in a certain interaction basis, which needs to be rotated to the mass basis. In this case, the matrices must be hermitian, idempotent ($\lambda^2 = \lambda$) and $\text{tr } \lambda = 1$ and, as explained in [19], can be parameterized by two complex numbers, $\alpha^{\ell,q}$ and $\beta^{\ell,q}$, in the following way:

$$\lambda^{\ell,q} = \frac{1}{1 + |\alpha^{\ell,q}|^2 + |\beta^{\ell,q}|^2} \begin{pmatrix} |\alpha^{\ell,q}|^2 & \alpha^{\ell,q}\bar{\beta}^{\ell,q} & \alpha^{\ell,q} \\ \bar{\alpha}^{\ell,q}\beta^{\ell,q} & |\beta^{\ell,q}|^2 & \beta^{\ell,q} \\ \bar{\alpha}^{\ell,q} & \bar{\beta}^{\ell,q} & 1 \end{pmatrix}. \quad (31)$$

In order to be consistent in our analysis, we must not restrict ourselves to the ratios $R_{D^{(*)}}$ and $R_{J/\psi}$. The first reason is that the Langrangian (30) directly contributes to many other physical observables, for example the previously mentioned $\text{BR}(B \rightarrow K^{(*)}\nu\bar{\nu})$ and even Lepton Flavour violating processes, like $B \rightarrow Ke^\pm\mu^\mp$, due to the off-diagonal terms of λ^ℓ . In addition, the running of the Renormalization Group equations causes the mixing of the operators in Lagrangian (30) with other SMEFT operators. For example, the insertion of $O_{\ell q(1)}$ ($O_{\ell q(3)}$) is necessary for the one loop corrections to $O_{\varphi q(1)}$ and $O_{\varphi \ell(1)}$ ($O_{\varphi q(3)}$ and $O_{\varphi \ell(3)}$) operators that are relevant for interactions between Z bosons and fermions. This justifies the need to perform global fits including various observables from B -physics and electroweak precision tests.

We have performed the fits including all observables implemented by **smelli** version 2.3.3 [60] plus $R_{J/\psi}$ ¹. The goodness of each fit is evaluated with its difference of χ^2 with respect to the SM, $\Delta\chi^2_{\text{SM}} = \chi^2_{\text{SM}} - \chi^2_{\text{fit}}$, being χ^2_{fit} as defined in (20). Besides, the package **smelli** computes the differences of the logarithms of the likelihood function as $\Delta \log L = -\frac{1}{2}\Delta\chi^2_{\text{SM}}$ and, in order to compare two fits A and B , we use the pull between them in units of σ , defined as [61]

$$\text{Pull}_{A \rightarrow B} = \sqrt{2} \text{Erf}^{-1}[F(\Delta\chi^2_A - \Delta\chi^2_B; n_B - n_A)], \quad (32)$$

where Erf^{-1} is the inverse of the error function, F is the cumulative distribution function of the χ^2 distribution and n is the number of degrees of freedom of each fit. The SM input parameters are chosen to be the same as in our previous work [19].

For comparison with our previous results, we have considered the two scenarios defined in [19] and, motivated by the tension in the new $B^+ \rightarrow K^+\nu\bar{\nu}$ measurement at Belle II [28] together with the alleviation of the tension in the $R_{K^{(*)}}$ ratios, we have introduced a new scenario called Scenario III:

- **Scenario I:** Includes only mixing between the second and third generations through β^ℓ and β^q , that is, $\alpha^\ell = \alpha^q = 0$ and $C_1 = C_3 \equiv C$.
- **Scenario II:** The only assumption is $C_1 = C_3 \equiv C$. Mixing with both first and second generation leptons through α^ℓ , β^ℓ , α^q and β^q is considered.
- **Scenario III:** C_1 and C_3 are independent parameters, and we do not consider mixing in the lepton sector, that is $\alpha^\ell = \beta^\ell = 0$.

¹We implemented the observable $R_{J/\psi}$ using the form factors in [51].

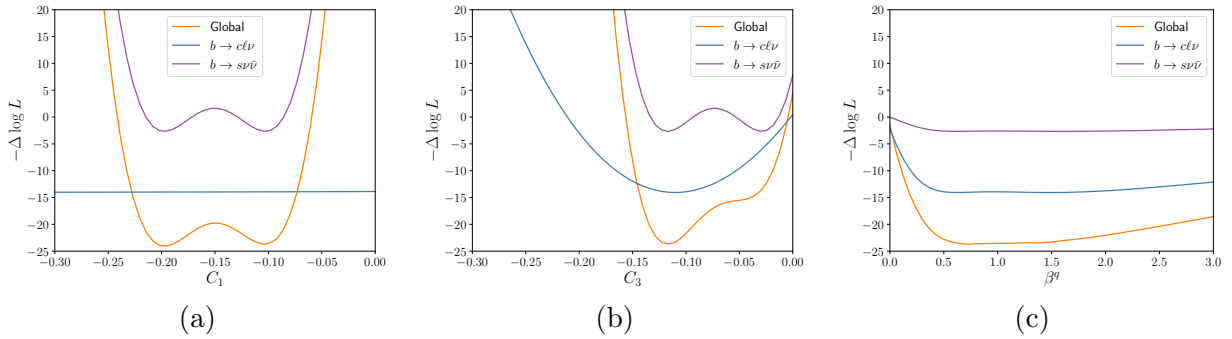


Figure 3: Negative of the logarithm of the likelihood function when varying (a) C_1 (b) C_3 and (c) β^q with respect to their values at the best fit for Scenario III.

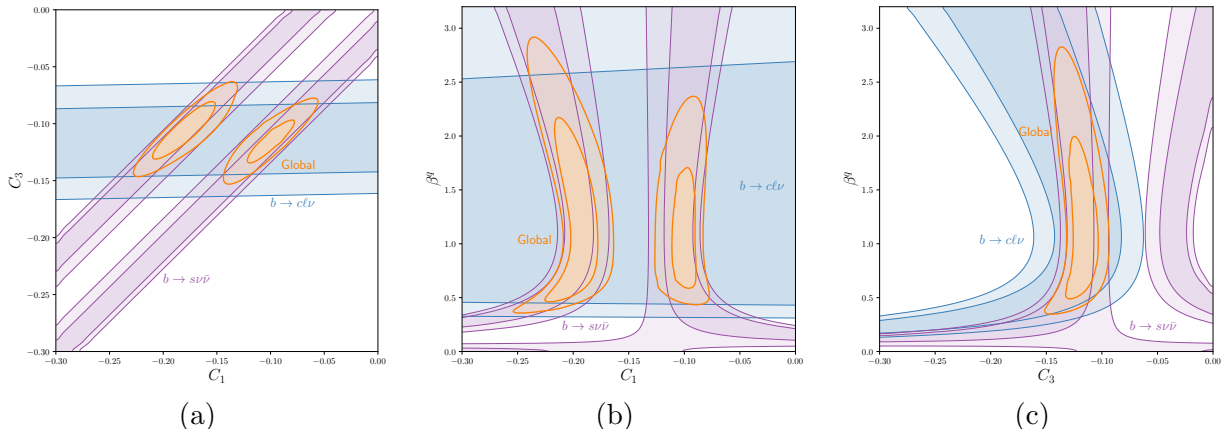


Figure 4: Regions of constant likelihood in Scenario III for (a) C_1 and C_3 plane (b) C_1 and β^q plane and (c) C_3 and β^q plane, with the rest of parameters as in the best fit point of Scenario III.

Scenarios I and II assumed that $C_1 = C_3 \equiv C$ because at that time, the $R_{K^{(*)}}$ observables presented deviations as compared to their SM predictions, while the constraints set by the $B \rightarrow K^{(*)}\nu\bar{\nu}$ decays were quite stringent. However, at present the experimental situation has reversed, with the tension in the $R_{K^{(*)}}$ ratios disappearing and a new anomaly appearing in $B^+ \rightarrow K^+\nu\bar{\nu}$, pointing towards different NP contributions to C_1 and C_3 . Scenario III assumes that C_1 and C_3 are independent parameters and. Additionally, since there are no longer discrepancies in muonic observables, we do not consider mixing in the lepton sector ($\alpha^\ell = \beta^\ell = 0$); we are also discarding mixing to the first quark generation since it played no role in our previous fits. In all three scenarios, only real values for the fit parameters are considered.

The results of the best fits to the rotation parameters and the coefficients C are summarized in Table 1. Scenarios I and II present a similar best fit point, with $C \sim -0.12$, $\beta^q = 0.8$ and the rest of the rotation parameters compatible with zero. The $\Delta\chi^2_{\text{SM}}$ is also similar, with $\Delta\chi^2_{\text{SM}} = 39.8$ in Scenario I and $\Delta\chi^2_{\text{SM}} = 43.1$ in Scenario II, which results in Scenario I having a better pull because there are less degrees of freedom, i.e. it is a simpler hypothesis. As anticipated, Scenario III results in a much better fit as compared to Scenarios I and II, since it requires the minimum number of parameters needed to describe simultaneously the anomalies in $R_{D^{(*)}}$ and $B \rightarrow K\nu\bar{\nu}$, with $\Delta\chi^2_{\text{SM}} = 46.66$ and a pull of 6.25σ .

In Scenario III, since $\alpha^\ell = \beta^\ell = 0$, there is no mixing in the leptonic sector, and the NP only affects the third generation, i.e., $\lambda_{33}^\ell = 1$ and $\lambda_{ij}^\ell = 0$ for all the other entries. Meanwhile, with a fit value of β^q close to one, there is a large mixing between the second and third quark generations, resulting in $\lambda_{22}^q = 0.29$, $\lambda_{33}^q = 0.71$ and $\lambda_{23}^q = \lambda_{32}^q = 0.45$. This mixing structure thus provides large contributions to $b \rightarrow s \nu_\tau \bar{\nu}_\tau$ and $b \rightarrow c \tau^- \bar{\nu}_\tau$ transitions while leaving $b \rightarrow s e^+ e^-$ and $b \rightarrow s \mu^+ \mu^-$ unaltered at tree level.

The role of each parameter of the fit in constraining each class of observables is shown in Figures 3 and 4. The one-dimensional slices of the likelihood function for Scenario III is included in Figure 3.

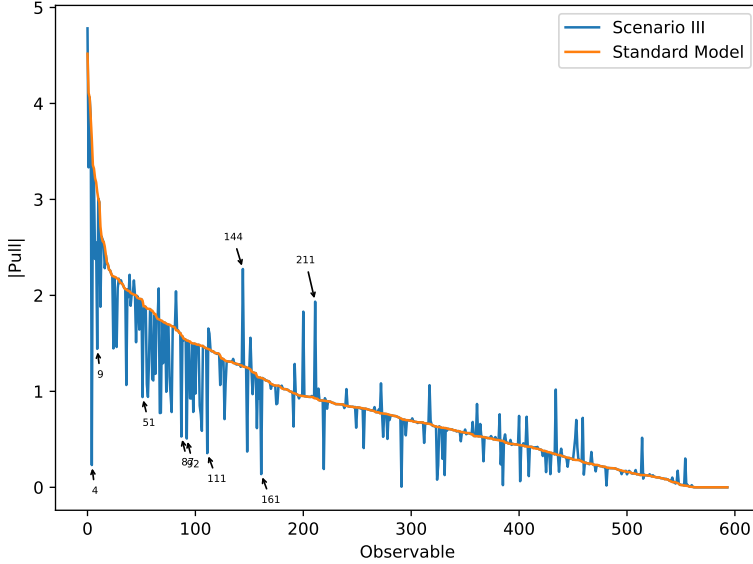


Figure 5: Pull of the observables considered for the global fit in the SM (orange line) and Scenario III (blue line). The observables are ordered by decreasing SM pull, and the ones in which the SM and Scenario III differ more than 1σ are specially marked.

The global fit (in orange) consists of 593 observables listed in Appendix A. However, it can be seen that it is largely dominated by the two classes of observables that we have been discussing in the previous sections: $b \rightarrow c\ell\nu$ (in blue) and $b \rightarrow s\nu\bar{\nu}$ (in purple). In particular, the $b \rightarrow s\nu\bar{\nu}$ observables determine the likelihood function in the direction of the parameter C_1 , both $b \rightarrow c\ell\nu$ and $b \rightarrow s\nu\bar{\nu}$ contribute to the likelihood function in the direction of C_3 , and $b \rightarrow c\ell\nu$ observables present the most important contribution to the likelihood in the direction of β^q . A similar picture emerges in Figure 4 when the contours of constant likelihood are considered. As indicated by the matching conditions in Eqs (19) and (27), the Wilson coefficient C_{VL} relevant for the $b \rightarrow c\ell\nu$ decays depends on $C_{\ell q(3)}^{3323} = C_3 \lambda_{23}^q$ while the coefficient C_L^{33} of the $b \rightarrow s\nu\bar{\nu}$ observables depends on both $C_{\ell q(1)}^{3323} = C_1 \lambda_{23}^q$ and $C_{\ell q(3)}^{3323} = C_3 \lambda_{23}^q$.

After applying the running of the Renormalization Group equation and the matching conditions (see [19] for details), the Wilson coefficients relevant for the $b \rightarrow c\tau^-\bar{\nu}_\tau$ and $b \rightarrow s\nu_\tau\bar{\nu}_\tau$ processes at the scale $\mu = m_b$ are

$$C_{VL} = 0.089, \quad C_L^{33} = 0.61, \quad (33)$$

while the other coefficients in Eq. (19) and Eq. (27) do not receive contributions from Scenario III. There is also a contribution to the Wilson coefficient C_9^ℓ which enters the $b \rightarrow s\ell^+\ell^-$ decays for $\ell = e, \mu$ [19, 62]. Since this contribution is generated radiatively from C_9^τ , it is lepton flavour universal for the light flavours, $C_9^e = C_9^\mu = -0.58$, and consequently it does not affect the $R_{K^{(*)}}$ ratios, which remain at their SM values $R_{K^{(*)}} \approx 1$. However, this contribution does enter in the branching ratios of $B \rightarrow K^{(*)}\mu^+\mu^-$ and $B_s \rightarrow \phi\mu^+\mu^-$.

The predictions for all the observables included in the fit, as well as the pull in the SM and in Scenario III (NP pull), are given in Appendix A. Figure 5 shows the comparison of the pull of each observable with respect to their experimental value in the SM (orange line) and in the Scenario III (blue line). Here the observables in which the SM and Scenario III differ more than 1σ are highlighted. We observe that the highlighted observables are all related to the B -meson anomalies: $R_{D^*}^\ell$ (observable 4) and R_D^ℓ (observable 92) improve by 3.3σ and 1σ respectively; $\text{BR}(B^+ \rightarrow K^+\nu\bar{\nu})$ (observable 9) improves by 1.7σ and $\text{BR}(B^+ \rightarrow K^{*+}\nu\bar{\nu})$ (observable 161) by 1σ while $\text{BR}(B^0 \rightarrow K^{*0}\nu\bar{\nu})$ (observable 144) gets worse by 1σ . And finally, regarding the branching ratios of $b \rightarrow s\mu^+\mu^-$ at high q^2 , $\text{BR}(B^\pm \rightarrow K^\pm\mu^+\mu^-)$ in the $[16 - 17]$ GeV 2 (observable 51) and $[15 - 22]$ GeV 2 (observable 87) bins, as well as $\text{BR}(B_s^\pm \rightarrow \phi^\pm\mu^+\mu^-)$ in the $[15 - 19]$ GeV 2 bin (observable 111), improve by around 1σ while $\text{BR}(B^\pm \rightarrow K^\pm\mu^+\mu^-)$ in the $[17 - 18]$ GeV 2 bin (observable 211) gets worse also by 1σ . As pointed out in Section 2.2, it is not possible to describe $B^+ \rightarrow K^+\nu\bar{\nu}$ and $B^0 \rightarrow K^{*0}\nu\bar{\nu}$ decays only with left-handed effective operators, consequently resulting in a worse pull for observable 144. As for

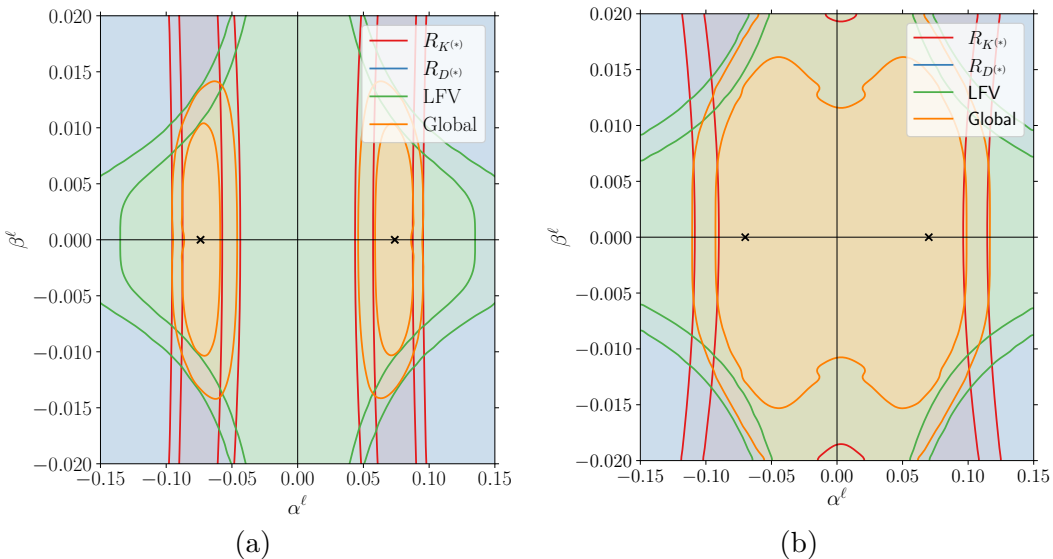


Figure 6: Regions of constant likelihood for α^ℓ and β^ℓ parameters in Scenario II as (a) in the previous work [19] and (b) in the current work.

the $B^+ \rightarrow K^+ \mu^+ \mu^-$ differential branching ratios, both LHCb [1] and CMS [18] find some tension between the $[17 - 18] \text{ GeV}^2$ bin, which is measured above the SM prediction, and the rest of the bins in the $q^2 \geq 15 \text{ GeV}^2$, which are below their SM prediction, and our fit reproduces said tension.

3.1 Comparison with previous results

The inclusion of the new experimental measurements at LHCb for $R_{K^{(*)}}$ [47, 63] has significantly impacted our global fit, as compared to previous results presented in [19]. In the previous fit, we found that a sizable contribution to α^ℓ was needed to describe the $R_{K^{(*)}}$ anomaly via NP affecting the electron decay mode. Now that the experimental measurements for $R_{K^{(*)}}$ are compatible with the SM predictions, the current fit no longer requires large deviations in α^ℓ . In consequence, there is no mixing in the leptonic sector, with $\lambda_{33}^\ell \approx 1$ affecting the tau decays (required to describe LFUV in $b \rightarrow c\tau\nu_\tau$ processes), while $\lambda_{ij}^\ell \approx 0$ for $ij \neq 33$. In the quark sector, the central values found by the fit present no significant changes as compared to the previous one, with large NP effects in β^q needed to describe the anomalies in flavour-changing $b \rightarrow c$ charged currents. However, we observe that β^q presents a larger allowed range, including even regions with $\beta^q > 1$, that is, with larger NP effects in the second generation than in the third generation. In the previous fit, β^q was constrained by the LFV decays $B \rightarrow K^{(*)}\mu e$, which received NP contributions through $C\lambda_{23}^q\lambda_{12}^\ell \sim C\beta^q\alpha^\ell\beta^\ell$. With the new fit preferring values of α^ℓ much closer to zero, the impact of β^q in the LFV observables is decreased, and instead, β^q is controlled mainly by the $b \rightarrow cl\nu$ decays.

This is illustrated in Figure 6, where the two-dimensional section of the likelihood function for the parameters α^ℓ - β^ℓ in Scenario II, with the rest of the parameters set at the best fit point of this scenario, is compared between the previous fit (left) and the new fit (right). In [19] we found that the better fit, with the inclusion of previous discrepancies on R_K and R_{K^*} results, corresponded to Scenario II. However, the present experimental measurements of these ratios do not have discrepancies with the SM predictions anymore. In fact, it can be seen that the main difference is the region allowed for the $R_{K^{(*)}}$ observables, inside the red lines: in the previous fit, the allowed region corresponded to $0.04 \leq |\alpha^\ell| \leq 0.10$, which was not compatible with the SM value $\alpha^\ell = 0$ owing to the experimental anomalies at that moment. On the other hand, the allowed region in the current fit is $0 \leq |\alpha^\ell| \leq 0.12$, which includes the SM point since the anomalies are gone. The global fit, in orange, follows the same logic.

The predictions for R_D , R_{D^*} and $R_{J/\psi}$ observables in the best fit points for Scenarios I, II and III are shown in Figure 7(a). R_D and R_{D^*} exhibit very similar values in both scenarios II and III (as $\alpha^{l,q}$ does not affect these predictions), and these fitted values align well with experimental results.

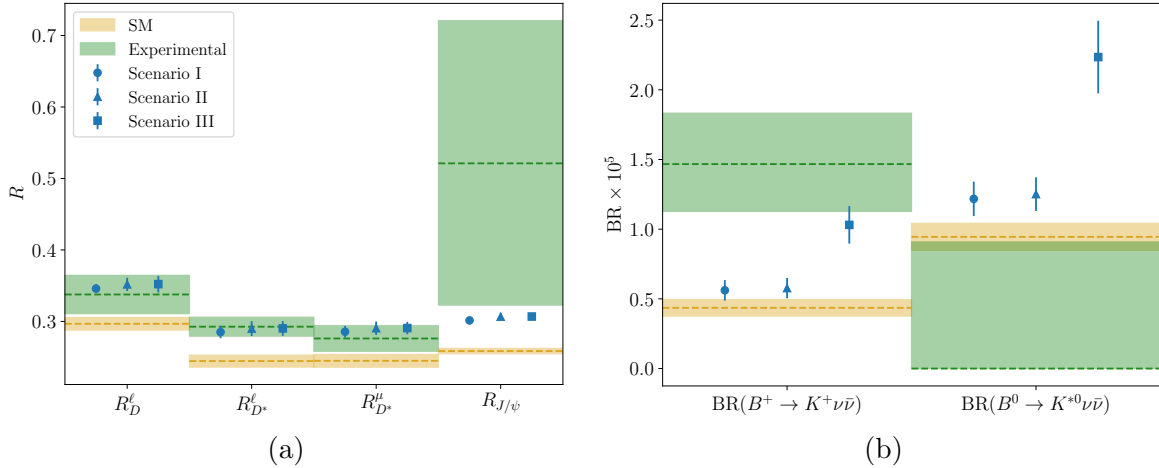


Figure 7: Predictions for selected (a) $b \rightarrow cl\nu$ LFU ratios and (b) $b \rightarrow sv\bar{\nu}$ branching ratios. The predictions in Scenarios I, II and III and their expected error are represented with blue markers. The SM prediction and its 1σ error are represented by the yellow regions. The experimental measurement and its 1σ error are represented by the green regions.

Observable	Previous fit	Current fit
$R_K^{[1.1, 6.0]}$	0.83 (0.28σ)	1.001 (1.1σ)
$R_{K^{*0}}^{[0.045, 1.1]}$	0.884 (2.1σ)	0.924 (0.026σ)
$R_{K^{*0}}^{[1.1, 6.0]}$	0.84 (1.4σ)	0.996 (0.41σ)
R_D^ℓ	0.351 (0.16σ)	0.344 (0.51σ)
$R_{D^*}^\ell$	0.290 (0.41σ)	0.283 (0.23σ)
$R_{D^*}^\mu$	0.290 (0.75σ)	0.284 (0.77σ)
$R_{J/\psi}$	-	0.306 (1.1σ)
$\text{BR}(B^+ \rightarrow K^+ \nu\bar{\nu})$	0.577×10^{-5} (1.1σ)	0.970×10^{-5} (1.4σ)
$\text{BR}(B^0 \rightarrow K^{*0} \nu\bar{\nu})$	1.252×10^{-5} (1.5σ)	2.104×10^{-5} (2.3σ)

Table 2: Comparison of the predictions for $b \rightarrow sl^+\ell^-$, $b \rightarrow cl\nu$ and $b \rightarrow sv\bar{\nu}$ observables between our previous fit and the current fit in Scenario II. The significance of the predictions in the column “Previous fit” are referred to the experimental measurements that were available in Ref. [19], while the significances in the column “Current fit” correspond to the updated values.

The current fit is largely dominated in the $b \rightarrow cl\nu$ sector by the $R_{D^{(*)}}$ ratios, as their uncertainty is much smaller than in the case of $R_{J/\psi}$. It would be therefore desirable to improve the measurements of $R_{J/\psi}$ in order to obtain an independent handle of the $b \rightarrow cl\nu$ sector and further clarify the present anomaly.

Figure 7(b) includes the predictions for $B^+ \rightarrow K^+ \nu\bar{\nu}$ and $B^0 \rightarrow K^{*0} \nu\bar{\nu}$ branching ratios. In both cases we can see how the scenario I and II, in which the coefficients $C_1 = C_3$ were not independent, fail to correctly capture the NP contribution, yielding values very close to the SM predictions. In contrast, Scenario III manages to improve the results in the charged sector, although the results in the neutral sector are worsened.

The comparison of the values obtained for $b \rightarrow sl^+\ell^-$, $b \rightarrow cl\nu$ and $b \rightarrow sv\bar{\nu}$ observables analyzed in this paper can be found in Table 2. The significance of the deviations with respect to the experimental values, in units of σ , is included for all observables. The ones in the column “Previous fit” are referred to the experimental measurements that were available in Ref. [19], while the ones in the column “Current fit” correspond to the updated values in this work. In the case of the $R_{K^{(*)}}$ ratios, the current fit improves the pull for $R_{K^{*0}}^{[1.1, 6.0]}$ and $R_{K^{*0}}^{[0.045, 1.1]}$, the later by almost 2σ . At the same time, the pull for $R_{K^+}^{[1.1, 6.0]}$ has increased to 1.1σ . The reason for this change is that this is the only bin where some of the tension with the SM prediction still survives, and our fit reproduces this tension. The

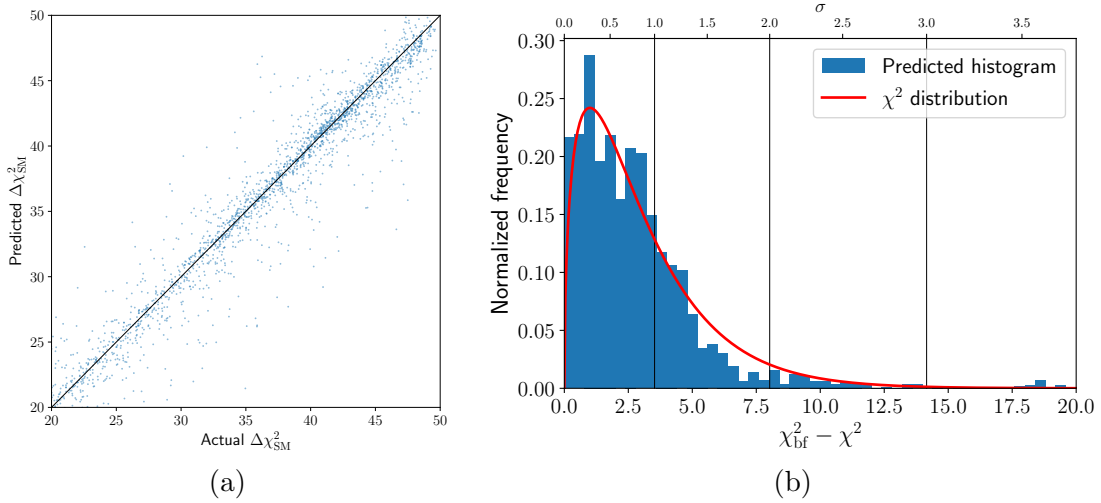


Figure 8: (a) Linear regression between the actual values of the $\Delta\chi^2_{\text{bf}}$ (horizontal axis) and the values predicted by the XGBoost model (vertical axis) in the validation set in Scenario III. (b) Histogram of the sample of points generated by the Machine Learning-based Monte Carlo algorithm in Scenario III, in blue, compared to the χ^2 probability distribution function, in red.

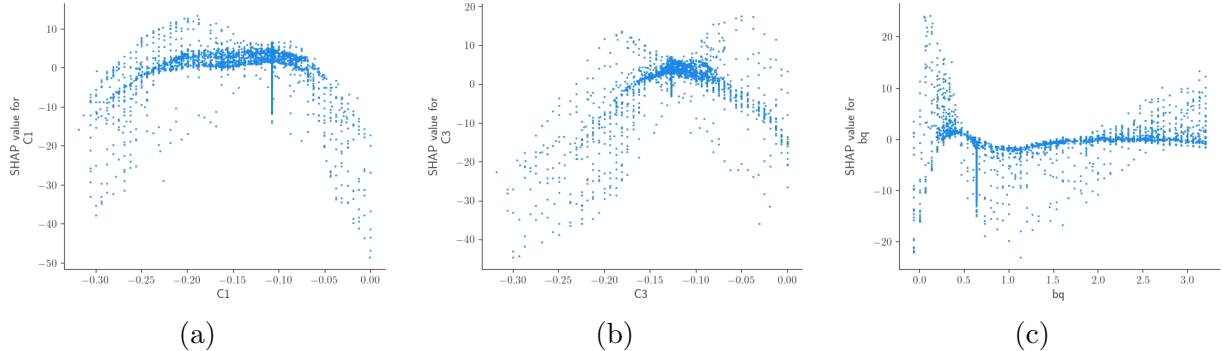


Figure 9: Distribution of SHAP values for each parameter of the fit: (a) C_1 , (b) C_3 , (c) β^q .

updated measurements of $R_{D^{(*)}}$ and the inclusion of the observable $R_{J/\psi}$ with its large uncertainty, have a lesser impact on our fit. However, for the $R_{D^{(*)}}$ ratio that includes the decay mode to electrons, $R_{D^{(*)}}^\ell$, this work marks an improvement over the previous fit due to the reduced NP effects in α^ℓ .

The impact of the new measurement and the reduced NP effects in α^ℓ can also be noticed in other $b \rightarrow se^+e^-$ observables, for example in the inclusive branching ratio $\text{BR}(B \rightarrow X_s e^+e^-)$, that has changed from 1.3σ to 1.6σ in the $[14.2, 25.0]\text{ GeV}^2$ bin (observable 113 in Appendix A) and from 0.23σ to 0.74σ in the $[1.0, 6.0]\text{ GeV}^2$ bin (observable 407). Also in LFU ratios, like other bins of $R_{K^{(*)}}$ that were measured by Belle [64], for example $R_{K^0}^{[4.0, 8.12]}$ changing from 0.86σ to 1.3σ (observable 140) and $R_{K^+}^{[4.0, 8.12]}$ from 1σ to 0.59σ (observable 343). By contrast, $b \rightarrow s\mu^+\mu^-$ observables like the angular observables P'_4 and P'_5 or the branching ratios $\text{BR}(B \rightarrow K^*\mu^+\mu^-)$ and $\text{BR}(B_s \rightarrow \phi\mu^+\mu^-)$ remain unchanged between both fits, because the value for β^ℓ has not changed.

3.2 Machine Learning analysis

In this section we summarize some details of the Machine Learning (ML) algorithm used in this work, by following the procedure explained in [19]. Since the obtained likelihood contours do not adhere to a Gaussian distribution, the ML algorithm is used to generate samples that match the obtained distributions. Besides, we use a Montecarlo analysis using Machine Learning to extract the confidence intervals and correlations between observables, as given in [19].

Using the XGBoost (eXtreme Gradient Boosting) algorithm we can train an ensemble of regression trees capable of approximating the log-likelihood function of our fit. We built a training sample of

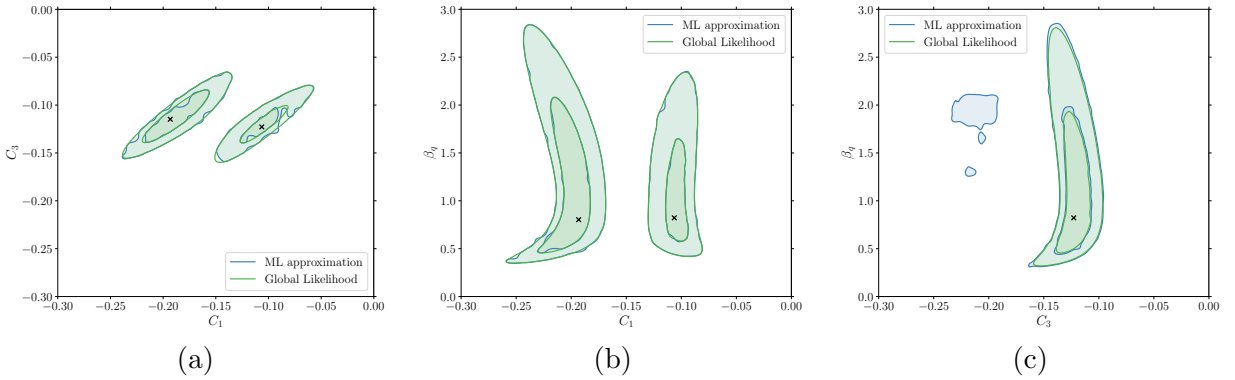


Figure 10: Comparison between the 1σ and 2σ likelihood contours obtained using the ML approximation (blue) and the actual contours (green) in (a) C_1 and C_3 plane, (b) C_1 and β^q plane and (c) C_3 and β^q plane.

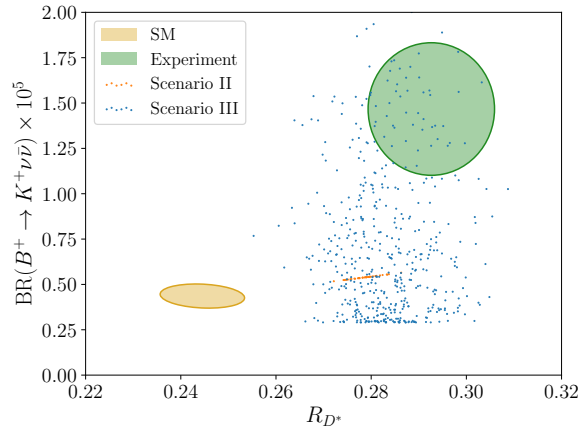


Figure 11: Values of the observables R_{D^*} and $\text{BR}(B^+ \rightarrow K^+ \nu \bar{\nu})$ in the ML-generated samples for scenario II (orange points) and scenario III (blue points), compared to the SM prediction (yellow region) and experimental measurement (green region).

5,000 parameter points with their corresponding likelihood values and split it into two parts: 50% of the points for training and 50% of the points for validation of the model. We train the ML model with a learning rate of 0.03 and allow early stopping after 5 rounds of stagnant learning. The training process finalized after 860 boosting rounds.

The correlation between the actual values of the χ^2_{SM} in the validation dataset and the corresponding predictions by the ML model is included in Figure 8(a) for Scenario III. The Pearson coefficient for linear correlation is $r = 0.96$, indicating an excellent agreement. The histogram for the predicted χ^2 values in Figure 8(b) shows how, once again, the ML-generated points closely follow the general shape of the χ^2 distribution.

After training the model and generating a sample of points using a Machine Learning Montecarlo algorithm, we plotted the logarithm of the likelihood while varying different parameters, as shown in Figure 9. Note that the parameters follow the shapes obtained in the global fit as presented in Figure 3 (with negative sign). The columns of dots visible in the three plots result from an over-representation of the best-fit points in the data sets for $C_1 = -0.11$, $C_3 = -0.12$ or $\beta^q = 0.6$. This effect arises from using a combination of two different data sets: one with randomly generated points across the parameter space, and another with points in a grid used for the elaboration of Figure 4. In the latter, each pair of parameters is sampled while keeping the remaining parameter fixed at its best-fit value. We also obtained the contours depicted in Figure 10, showing a high degree of agreement with the contours obtained in the fit. Therefore, we can conclude that ML, made jointly with the SHAP values, reproduce correctly the general features of the fit and it's a suitable strategy for this kind of analysis.

Finally, it is worth mentioning that in [19] we determined the predictions of our model for several

selected observables of various flavour sectors, including the R_{D^*} observables and $B^+ \rightarrow K^+\nu\bar{\nu}$ decay. The results showed an almost-perfect correlation for these two observables. The predictions for these two observables in the generated sample were shown in Figure 12 of [19]. With the inclusion of the new experimental results on R_{D^*} ratios at Belle II [16] and our new Scenario III, in which the Wilson coefficients C_1 and C_3 are independent parameters and not mixing in the lepton sector is considered, our previous results change drastically. Predictions for these two observables in the ML-generated samples for Scenario II (as in the previous paper) and Scenario III are shown in Figure 11, where we can observe how the correlation present in Scenario II disappears in Scenario III. Building a UV complete model reproducing the interplay between R_{D^*} and $\text{BR}(B^+ \rightarrow K^+\nu\bar{\nu})$ in Figure 11 is out of the scope of this work. However there are some proposals in the literature that describe the $R_{D^{(*)}}$ anomalies while enhancing $\text{BR}(B^+ \rightarrow K^+\nu\bar{\nu})$ with vector leptoquarks [65, 66], non-universal Z' bosons [67] or combinations of scalars and fermions [68].

4 Conclusions

In this paper we have performed an improved analysis of the anomalies in B -meson decays by using an effective field theory approach and considering the NP effects on the Wilson coefficients of the effective Lagrangian. The latest experimental results of R_K ratios, in agreement with the SM, and the new deviation observed on $B^+ \rightarrow K^+\nu\bar{\nu}$ decay at Belle II are included in the global fits. Consequently, a new scenario (Scenario III) is considered in the present study, with only mixing between the second and third quark generations and no mixing in the lepton sector, being the Wilson coefficients for the singlet and triplet four fermion effective operators independent. Both the recent experimental measurements of $\text{BR}(B^+ \rightarrow K^+\nu\bar{\nu})$ and $R_{J/\psi}$ are included in the analysis. Besides, branching ratios associated with $B \rightarrow D^{(*)}\tau\nu$ decays are considered. The fact that the global fit is dominated by these classes of observables underlines their potential as probes to NP. All these ingredients have led to a marked improvement in our results compared to the previous study in [19], in which a global fit to experimental data available at that time was performed, with the inclusion of anomalies on the ratios of branching fractions for the $b \rightarrow s\ell^+\ell^-$ processes, R_K and R_{K^*} .

We use a Machine Learning (ML) algorithm in our analysis, by checking the agreement between the results obtained for this procedure and both the general shape of the $\Delta\chi^2$ distribution and the analysis of the impact of each parameter on the global fit. In our Scenario III, the $B \rightarrow K^{(*)}\nu\bar{\nu}$ observables constrain the parameter C_1 , both $B \rightarrow D^{(*)}\ell\nu$ and $B \rightarrow K^{(*)}\nu\bar{\nu}$ constrain C_3 , and $B \rightarrow D^{(*)}\ell\nu$ observables present the most important constraint to β^q .

The results of the global fit after including a wide range of flavour and electroweak observables are displayed in Table 1, and the predictions for the most relevant observables are summarized in Table 2. The comparison with the previous scenarios considered in [19] is included in the discussion. Our results show that Scenario III, which introduces independent parameters C_1 and C_3 without mixing in the lepton sector, provides the best fit to experimental results, achieving a pull of 6.25σ . This scenario successfully accounts for the discrepancies observed in R_{D^*} and $R_{J/\psi}$ measurements while maintaining consistency with the Standard Model in the R_K ratios. Furthermore, it improves the predicted branching ratio for $\text{BR}(B^+ \rightarrow K^+\nu\bar{\nu})$ although it does not fully explain $\text{BR}(B^0 \rightarrow K^{*0}\nu\bar{\nu})$. The results are pointing in the direction of NP that interacts mainly with the third generation of leptons, reminiscent of the $U(2)$ flavour symmetry hypothesis [69, 70]. The situation would be clarified further with measurements of $R_{J/\psi}$ achieving a resolution similar to that of $R_{D^{(*)}}$, and with additional τ observables, for example the longitudinal polarisation in $B_c \rightarrow J/\psi\tau\nu$ or the branching ratio of $B \rightarrow K^{(*)}\tau^+\tau^-$.

Acknowledgments

This work is partially supported by Spanish MINECO/FEDER Grants No. PGC2022-126078NB-C21 funded by MCIN/AEI/10.13039/ 501100011033 and “ERDF A way of making Europe” and Grant DGA-FSE Grant 2020-E21-17R Aragón Government and the European Union - NextGenerationEU Recovery and Resilience Program on *Astrofísica y Física de Altas Energías* CEFCA-CAPA-

ITAINNOVA. Additionally, J.A has received funding from the Fundación Ramón Areces “Beca para ampliación de estudios en el extranjero en el campo de las Ciencias de la Vida y de la Materia”.

References

- [1] **LHCb** Collaboration, R. Aaij *et al.*, “Differential branching fractions and isospin asymmetries of $B \rightarrow K^{(*)}\mu^+\mu^-$ decays,” *JHEP* **06** (2014) 133, [arXiv:1403.8044 \[hep-ex\]](https://arxiv.org/abs/1403.8044).
- [2] **LHCb** Collaboration, R. Aaij *et al.*, “Test of lepton universality using $B^+ \rightarrow K^+\ell^+\ell^-$ decays,” *Phys. Rev. Lett.* **113** (2014) 151601, [arXiv:1406.6482 \[hep-ex\]](https://arxiv.org/abs/1406.6482).
- [3] **LHCb** Collaboration, R. Aaij *et al.*, “Angular analysis and differential branching fraction of the decay $B_s^0 \rightarrow \phi\mu^+\mu^-$,” *JHEP* **09** (2015) 179, [arXiv:1506.08777 \[hep-ex\]](https://arxiv.org/abs/1506.08777).
- [4] **LHCb** Collaboration, R. Aaij *et al.*, “Angular analysis of the $B^0 \rightarrow K^{*0}\mu^+\mu^-$ decay using 3 fb^{-1} of integrated luminosity,” *JHEP* **02** (2016) 104, [arXiv:1512.04442 \[hep-ex\]](https://arxiv.org/abs/1512.04442).
- [5] **LHCb** Collaboration, R. Aaij *et al.*, “Measurements of the S-wave fraction in $B^0 \rightarrow K^+\pi^-\mu^+\mu^-$ decays and the $B^0 \rightarrow K^*(892)^0\mu^+\mu^-$ differential branching fraction,” *JHEP* **11** (2016) 047, [arXiv:1606.04731 \[hep-ex\]](https://arxiv.org/abs/1606.04731). [Erratum: JHEP 04, 142 (2017)].
- [6] **CMS, LHCb** Collaboration, V. Khachatryan *et al.*, “Observation of the rare $B_s^0 \rightarrow \mu^+\mu^-$ decay from the combined analysis of CMS and LHCb data,” *Nature* **522** (2015) 68–72, [arXiv:1411.4413 \[hep-ex\]](https://arxiv.org/abs/1411.4413).
- [7] **LHCb** Collaboration, R. Aaij *et al.*, “Measurement of the ratio of branching fractions $\mathcal{B}(\bar{B}^0 \rightarrow D^{*+}\tau^-\bar{\nu}_\tau)/\mathcal{B}(\bar{B}^0 \rightarrow D^{*+}\mu^-\bar{\nu}_\mu)$,” *Phys. Rev. Lett.* **115** no. 11, (2015) 111803, [arXiv:1506.08614 \[hep-ex\]](https://arxiv.org/abs/1506.08614). [Erratum: Phys.Rev.Lett. 115, 159901 (2015)].
- [8] **LHCb** Collaboration, R. Aaij *et al.*, “Measurement of the phase difference between short- and long-distance amplitudes in the $B^+ \rightarrow K^+\mu^+\mu^-$ decay,” *Eur. Phys. J. C* **77** no. 3, (2017) 161, [arXiv:1612.06764 \[hep-ex\]](https://arxiv.org/abs/1612.06764).
- [9] **LHCb** Collaboration, R. Aaij *et al.*, “Measurement of the $B_s^0 \rightarrow \mu^+\mu^-$ branching fraction and effective lifetime and search for $B^0 \rightarrow \mu^+\mu^-$ decays,” *Phys. Rev. Lett.* **118** no. 19, (2017) 191801, [arXiv:1703.05747 \[hep-ex\]](https://arxiv.org/abs/1703.05747).
- [10] **LHCb** Collaboration, R. Aaij *et al.*, “Search for the decays $B_s^0 \rightarrow \tau^+\tau^-$ and $B^0 \rightarrow \tau^+\tau^-$,” *Phys. Rev. Lett.* **118** no. 25, (2017) 251802, [arXiv:1703.02508 \[hep-ex\]](https://arxiv.org/abs/1703.02508).
- [11] **LHCb** Collaboration, R. Aaij *et al.*, “Test of lepton universality with $B^0 \rightarrow K^{*0}\ell^+\ell^-$ decays,” *JHEP* **08** (2017) 055, [arXiv:1705.05802 \[hep-ex\]](https://arxiv.org/abs/1705.05802).
- [12] **LHCb** Collaboration, R. Aaij *et al.*, “Measurement of the ratio of the $B^0 \rightarrow D^{*-}\tau^+\nu_\tau$ and $B^0 \rightarrow D^{*-}\mu^+\nu_\mu$ branching fractions using three-prong τ -lepton decays,” *Phys. Rev. Lett.* **120** no. 17, (2018) 171802, [arXiv:1708.08856 \[hep-ex\]](https://arxiv.org/abs/1708.08856).
- [13] **LHCb** Collaboration, R. Aaij *et al.*, “Evidence for the decay $B_S^0 \rightarrow \overline{K}^{*0}\mu^+\mu^-$,” *JHEP* **07** (2018) 020, [arXiv:1804.07167 \[hep-ex\]](https://arxiv.org/abs/1804.07167).
- [14] **LHCb** Collaboration, R. Aaij *et al.*, “Search for lepton-universality violation in $B^+ \rightarrow K^+\ell^+\ell^-$ decays,” *Phys. Rev. Lett.* **122** no. 19, (2019) 191801, [arXiv:1903.09252 \[hep-ex\]](https://arxiv.org/abs/1903.09252).
- [15] **CMS** Collaboration, C. Collaboration, “Test of lepton flavor universality violation in semileptonic B_c^+ meson decays at CMS,” . <https://cds.cern.ch/record/2868988>.
- [16] **Belle-II** Collaboration, I. Adachi *et al.*, “Test of lepton flavor universality with a measurement of $R(D^*)$ using hadronic B tagging at the Belle II experiment,” *Phys. Rev. D* **110** no. 7, (2024) 072020, [arXiv:2401.02840 \[hep-ex\]](https://arxiv.org/abs/2401.02840).

- [17] **LHCb** Collaboration, R. Aaij *et al.*, “Measurement of the branching fraction ratios $R(D^+)$ and $R(D^{*+})$ using muonic τ decays,” [arXiv:2406.03387 \[hep-ex\]](https://arxiv.org/abs/2406.03387).
- [18] **CMS** Collaboration, A. Hayrapetyan *et al.*, “Test of lepton flavor universality in $B^\pm \rightarrow K^\pm \mu^+ \mu^-$ and $B^\pm \rightarrow K^\pm e^+ e^-$ decays in proton-proton collisions at $\sqrt{s} = 13$ TeV,” *Rept. Prog. Phys.* **87** no. 7, (2024) 077802, [arXiv:2401.07090 \[hep-ex\]](https://arxiv.org/abs/2401.07090).
- [19] J. Alda, J. Guasch, and S. Penaranda, “Using Machine Learning techniques in phenomenological studies on flavour physics,” *JHEP* **07** (2022) 115, [arXiv:2109.07405 \[hep-ph\]](https://arxiv.org/abs/2109.07405).
- [20] J. Alda, J. Guasch, and S. Penaranda, “Anomalies in B mesons decays: Present status and future collider prospects,” in *International Workshop on Future Linear Colliders*. 5, 2021. [arXiv:2105.05095 \[hep-ph\]](https://arxiv.org/abs/2105.05095).
- [21] J. Alda, J. Guasch, and S. Penaranda, “Anomalies in B mesons decays: a phenomenological approach,” *Eur. Phys. J. Plus* **137** no. 2, (2022) 217, [arXiv:2012.14799 \[hep-ph\]](https://arxiv.org/abs/2012.14799).
- [22] J. Alda Gallo, J. Guasch, and S. Penaranda, “Exploring B-physics anomalies at colliders,” *PoS EPS-HEP2021* (2022) 494, [arXiv:2110.12240 \[hep-ph\]](https://arxiv.org/abs/2110.12240).
- [23] S. Jaiswal, S. Nandi, and S. K. Patra, “Extraction of $|V_{cb}|$ from $B \rightarrow D^{(*)}\ell\nu_\ell$ and the Standard Model predictions of $R(D^{(*)})$,” *JHEP* **12** (2017) 060, [arXiv:1707.09977 \[hep-ph\]](https://arxiv.org/abs/1707.09977).
- [24] “Heavy flavor averaging group.” 2024. <https://hflav-eos.web.cern.ch/hflav-eos/semi/moriond24/html/RDsDsstar/RDRDs.html>.
- [25] R.-Y. Tang, Z.-R. Huang, C.-D. Lü, and R. Zhu, “Scrutinizing new physics in semi-leptonic $B_c \rightarrow J/\psi \tau \nu$ decay,” *J. Phys. G* **49** no. 11, (2022) 115003, [arXiv:2204.04357 \[hep-ph\]](https://arxiv.org/abs/2204.04357).
- [26] **LHCb** Collaboration, R. Aaij *et al.*, “Measurement of the ratio of branching fractions $\mathcal{B}(B_c^+ \rightarrow J/\psi \tau^+ \nu_\tau)/\mathcal{B}(B_c^+ \rightarrow J/\psi \mu^+ \nu_\mu)$,” *Phys. Rev. Lett.* **120** no. 12, (2018) 121801, [arXiv:1711.05623 \[hep-ex\]](https://arxiv.org/abs/1711.05623).
- [27] S. Iguro, T. Kitahara, and R. Watanabe, “Global fit to $b \rightarrow c \tau \nu$ anomalies as of Spring 2024,” *Phys. Rev. D* **110** no. 7, (2024) 075005, [arXiv:2405.06062 \[hep-ph\]](https://arxiv.org/abs/2405.06062).
- [28] **Belle-II** Collaboration, I. Adachi *et al.*, “Evidence for $B \rightarrow K + \nu \nu^-$ decays,” *Phys. Rev. D* **109** no. 11, (2024) 112006, [arXiv:2311.14647 \[hep-ex\]](https://arxiv.org/abs/2311.14647).
- [29] R. Bause, H. Gisbert, and G. Hiller, “Implications of an enhanced $B \rightarrow K \nu \nu^-$ branching ratio,” *Phys. Rev. D* **109** no. 1, (2024) 015006, [arXiv:2309.00075 \[hep-ph\]](https://arxiv.org/abs/2309.00075).
- [30] **Belle** Collaboration, J. Grygier *et al.*, “Search for $B \rightarrow h \nu \bar{\nu}$ decays with semileptonic tagging at Belle,” *Phys. Rev. D* **96** no. 9, (2017) 091101, [arXiv:1702.03224 \[hep-ex\]](https://arxiv.org/abs/1702.03224). [Addendum: *Phys. Rev. D* 97, 099902 (2018)].
- [31] R. Bause, H. Gisbert, M. Golz, and G. Hiller, “Interplay of dineutrino modes with semileptonic rare B-decays,” *JHEP* **12** (2021) 061, [arXiv:2109.01675 \[hep-ph\]](https://arxiv.org/abs/2109.01675).
- [32] L. Calibbi, A. Crivellin, and T. Ota, “Effective Field Theory Approach to $b \rightarrow s \ell \ell^{(\prime)}$, $B \rightarrow K^{(*)} \nu \bar{\nu}$ and $B \rightarrow D^{(*)} \tau \nu$ with Third Generation Couplings,” *Phys. Rev. Lett.* **115** (2015) 181801, [arXiv:1506.02661 \[hep-ph\]](https://arxiv.org/abs/1506.02661).
- [33] B. Capdevila, A. Crivellin, S. Descotes-Genon, J. Matias, and J. Virto, “Patterns of New Physics in $b \rightarrow s \ell^+ \ell^-$ transitions in the light of recent data,” *JHEP* **01** (2018) 093, [arXiv:1704.05340 \[hep-ph\]](https://arxiv.org/abs/1704.05340).
- [34] A. Celis, J. Fuentes-Martin, A. Vicente, and J. Virto, “Gauge-invariant implications of the LHCb measurements on lepton-flavor nonuniversality,” *Phys. Rev. D* **96** no. 3, (2017) 035026, [arXiv:1704.05672 \[hep-ph\]](https://arxiv.org/abs/1704.05672).

- [35] A. K. Alok, B. Bhattacharya, A. Datta, D. Kumar, J. Kumar, and D. London, “New Physics in $b \rightarrow s\mu^+\mu^-$ after the Measurement of R_{K^*} ,” *Phys. Rev. D* **96** no. 9, (2017) 095009, [arXiv:1704.07397 \[hep-ph\]](#).
- [36] J. E. Camargo-Molina, A. Celis, and D. A. Faroughy, “Anomalies in Bottom from new physics in Top,” *Phys. Lett. B* **784** (2018) 284–293, [arXiv:1805.04917 \[hep-ph\]](#).
- [37] A. Datta, J. Kumar, and D. London, “The B anomalies and new physics in $b \rightarrow se^+e^-$,” *Phys. Lett. B* **797** (2019) 134858, [arXiv:1903.10086 \[hep-ph\]](#).
- [38] J. Aebischer, W. Altmannshofer, D. Guadagnoli, M. Reboud, P. Stangl, and D. M. Straub, “ B -decay discrepancies after Moriond 2019,” *Eur. Phys. J. C* **80** no. 3, (2020) 252, [arXiv:1903.10434 \[hep-ph\]](#).
- [39] R. Aoude, T. Hurth, S. Renner, and W. Shepherd, “The impact of flavour data on global fits of the MFV SMEFT,” *JHEP* **12** (2020) 113, [arXiv:2003.05432 \[hep-ph\]](#).
- [40] M. Algueró, J. Matias, B. Capdevila, and A. Crivellin, “Disentangling lepton flavor universal and lepton flavor universality violating effects in $b \rightarrow s\ell^+\ell^-$ transitions,” *Phys. Rev. D* **105** no. 11, (2022) 113007, [arXiv:2205.15212 \[hep-ph\]](#).
- [41] N. R. Singh Chundawat, “ CP violation in $b \rightarrow s\ell\ell$: a model independent analysis,” *Phys. Rev. D* **107** (2023) 075014, [arXiv:2207.10613 \[hep-ph\]](#).
- [42] C. Grunwald, G. Hiller, K. Kröninger, and L. Nollen, “More synergies from beauty, top, Z and Drell-Yan measurements in SMEFT,” *JHEP* **11** (2023) 110, [arXiv:2304.12837 \[hep-ph\]](#).
- [43] R. Bartocci, A. Biekötter, and T. Hurth, “A global analysis of the SMEFT under the minimal MFV assumption,” *JHEP* **05** (2024) 074, [arXiv:2311.04963 \[hep-ph\]](#).
- [44] N. Elmer, M. Madigan, T. Plehn, and N. Schmal, “Staying on Top of SMEFT-Likelihood Analyses,” [arXiv:2312.12502 \[hep-ph\]](#).
- [45] B. Capdevila, A. Crivellin, and J. Matias, “Review of semileptonic B anomalies,” *Eur. Phys. J. ST* **1** (2023) 20, [arXiv:2309.01311 \[hep-ph\]](#).
- [46] C. Grunwald, G. Hiller, K. Kröninger, and L. Nollen, “Predicting $B(B \rightarrow K^{(*)}\nu\bar{\nu})$ within the MFV-SMEFT using B , Top, Z and Drell-Yan data,” *PoS EPS-HEP2023* (2024) 298.
- [47] **LHCb** Collaboration, R. Aaij *et al.*, “Test of lepton universality in $b \rightarrow s\ell^+\ell^-$ decays,” *Phys. Rev. Lett.* **131** no. 5, (2023) 051803, [arXiv:2212.09152 \[hep-ex\]](#).
- [48] A. J. Buras, “Weak Hamiltonian, CP violation and rare decays,” in *Les Houches Summer School in Theoretical Physics, Session 68: Probing the Standard Model of Particle Interactions*, pp. 281–539. 6, 1998. [arXiv:hep-ph/9806471](#).
- [49] J. Aebischer, A. Crivellin, M. Fael, and C. Greub, “Matching of gauge invariant dimension-six operators for $b \rightarrow s$ and $b \rightarrow c$ transitions,” *JHEP* **05** (2016) 037, [arXiv:1512.02830 \[hep-ph\]](#).
- [50] J. Aebischer, M. Fael, C. Greub, and J. Virto, “B physics Beyond the Standard Model at One Loop: Complete Renormalization Group Evolution below the Electroweak Scale,” *JHEP* **09** (2017) 158, [arXiv:1704.06639 \[hep-ph\]](#).
- [51] **HPQCD** Collaboration, J. Harrison, C. T. H. Davies, and A. Lytle, “ $B_c \rightarrow J/\psi$ form factors for the full q^2 range from lattice QCD,” *Phys. Rev. D* **102** no. 9, (2020) 094518, [arXiv:2007.06957 \[hep-lat\]](#).
- [52] M. Tanaka and R. Watanabe, “New physics in the weak interaction of $\bar{B} \rightarrow D^{(*)}\tau\bar{\nu}$,” *Phys. Rev. D* **87** no. 3, (2013) 034028, [arXiv:1212.1878 \[hep-ph\]](#).

- [53] Y. Sakaki, M. Tanaka, A. Tayduganov, and R. Watanabe, “Testing leptoquark models in $\bar{B} \rightarrow D^{(*)}\tau\bar{\nu}$,” *Phys. Rev. D* **88** no. 9, (2013) 094012, [arXiv:1309.0301 \[hep-ph\]](#).
- [54] B. Grzadkowski, M. Iskrzynski, M. Misiak, and J. Rosiek, “Dimension-Six Terms in the Standard Model Lagrangian,” *JHEP* **10** (2010) 085, [arXiv:1008.4884 \[hep-ph\]](#).
- [55] E. E. Jenkins, A. V. Manohar, and P. Stoffer, “Low-Energy Effective Field Theory below the Electroweak Scale: Operators and Matching,” *JHEP* **03** (2018) 016, [arXiv:1709.04486 \[hep-ph\]](#).
- [56] J. Brod, M. Gorbahn, and E. Stamou, “Updated Standard Model Prediction for $K \rightarrow \pi\nu\bar{\nu}$ and ϵ_K ,” *PoS BEAUTY2020* (2021) 056, [arXiv:2105.02868 \[hep-ph\]](#).
- [57] F. Feruglio, P. Paradisi, and A. Pattori, “On the Importance of Electroweak Corrections for B Anomalies,” *JHEP* **09** (2017) 061, [arXiv:1705.00929 \[hep-ph\]](#).
- [58] C. Cornellà, F. Feruglio, and P. Paradisi, “Low-energy Effects of Lepton Flavour Universality Violation,” *JHEP* **11** (2018) 012, [arXiv:1803.00945 \[hep-ph\]](#).
- [59] F. Feruglio, “B-anomalies related to leptons and lepton flavour violation: new directions in model building,” *PoS BEAUTY2018* (2018) 029, [arXiv:1808.01502 \[hep-ph\]](#).
- [60] J. Aebrischer, J. Kumar, P. Stangl, and D. M. Straub, “A Global Likelihood for Precision Constraints and Flavour Anomalies,” *Eur. Phys. J. C* **79** no. 6, (2019) 509, [arXiv:1810.07698 \[hep-ph\]](#).
- [61] B. Capdevila, U. Laa, and G. Valencia, “Anatomy of a six-parameter fit to the $b \rightarrow s\ell^+\ell^-$ anomalies,” *Eur. Phys. J. C* **79** no. 6, (2019) 462, [arXiv:1811.10793 \[hep-ph\]](#).
- [62] A. Crivellin, C. Greub, D. Müller, and F. Saturnino, “Importance of Loop Effects in Explaining the Accumulated Evidence for New Physics in B Decays with a Vector Leptoquark,” *Phys. Rev. Lett.* **122** no. 1, (2019) 011805, [arXiv:1807.02068 \[hep-ph\]](#).
- [63] **LHCb** Collaboration, R. Aaij *et al.*, “Measurement of lepton universality parameters in $B^+ \rightarrow K^+\ell^+\ell^-$ and $B^0 \rightarrow K^{*0}\ell^+\ell^-$ decays,” *Phys. Rev. D* **108** no. 3, (2023) 032002, [arXiv:2212.09153 \[hep-ex\]](#).
- [64] **BELLE** Collaboration, S. Choudhury *et al.*, “Test of lepton flavor universality and search for lepton flavor violation in $B \rightarrow K\ell\ell$ decays,” *JHEP* **03** (2021) 105, [arXiv:1908.01848 \[hep-ex\]](#).
- [65] J. Fuentes-Martín, G. Isidori, M. König, and N. Selimović, “Vector Leptoquarks Beyond Tree Level III: Vector-like Fermions and Flavor-Changing Transitions,” *Phys. Rev. D* **102** (2020) 115015, [arXiv:2009.11296 \[hep-ph\]](#).
- [66] L. Allwicher, M. Bordone, G. Isidori, G. Piazza, and A. Stanzione, “Probing third-generation New Physics with $K \rightarrow \pi\nu\bar{\nu}$ and $B \rightarrow K^{(*)}\nu\bar{\nu}$,” [arXiv:2410.21444 \[hep-ph\]](#).
- [67] P. Athron, R. Martinez, and C. Sierra, “B meson anomalies and large $B^+ \rightarrow K^+\nu\bar{\nu}$ in non-universal $U(1)'$ models,” *JHEP* **02** (2024) 121, [arXiv:2308.13426 \[hep-ph\]](#).
- [68] G. Guedes and P. Olgoso, “From the EFT to the UV: the complete SMEFT one-loop dictionary,” [arXiv:2412.14253 \[hep-ph\]](#).
- [69] J. Fuentes-Martín, G. Isidori, J. Pagès, and K. Yamamoto, “With or without $U(2)$? Probing non-standard flavor and helicity structures in semileptonic B decays,” *Phys. Lett. B* **800** (2020) 135080, [arXiv:1909.02519 \[hep-ph\]](#).
- [70] D. A. Faroughy, G. Isidori, F. Wilsch, and K. Yamamoto, “Flavour symmetries in the SMEFT,” *JHEP* **08** (2020) 166, [arXiv:2005.05366 \[hep-ph\]](#).

A Pulls of the observables

The list of all observables that contribute to the global fit, as well as their prediction in Scenario III and their pull in both scenario III (NP pull) and SM is collected in this appendix. Observables are ordered according to their SM pull, and color-coded according to the difference between the scenario III and SM pulls, such that the observables with a better pull in scenario III are in green and red observables have a better pull in the SM.

Predictions for dimensionful observables are expressed in the corresponding power of GeV. The notation $\langle \dots \rangle$ means that the observable is binned in the invariant mass-squared of the di-lepton system q^2 , with the endpoints of the bin in GeV^2 given in the superscript. Accordingly, the notation $\frac{\langle \text{BR} \rangle}{\text{BR}}$ denotes a binned branching ratio normalised to the total branching ratio.

	Observable	NP prediction	NP pull	SM pull
0	$\langle \frac{d\text{BR}}{dq^2} \rangle (B^\pm \rightarrow K^\pm \mu^+ \mu^-)^{[19.24, 22.9]}$	5.5449×10^{-9}	4.8 σ	4.5 σ
1	$\langle \frac{d\text{BR}}{dq^2} \rangle (B_s \rightarrow \phi \mu^+ \mu^-)^{[2.5, 4.0]}$	4.6141×10^{-8}	3.3 σ	4.1 σ
2	$\langle \text{BR} \rangle (D^0 \rightarrow \pi^- e^+ \nu_e)^{[2, 2.98]}$	0.00022544	4.1 σ	4.1 σ
3	a_μ	0.0011659	3.8 σ	3.8 σ
4	$R_{\tau\ell}(B \rightarrow D^* \ell^+ \nu)$	0.28951	0.23 σ	3.6 σ
5	$\langle P_2 \rangle (B^0 \rightarrow K^{*0} \mu^+ \mu^-)^{[0.1, 0.98]}$	-0.13043	3.3 σ	3.4 σ
6	$\langle F_L \rangle (B^+ \rightarrow K^{*+} \mu^+ \mu^-)^{[2.5, 4]}$	0.77432	3.2 σ	3.3 σ
7	$\langle \frac{d\text{BR}}{dq^2} \rangle (B_s \rightarrow \phi \mu^+ \mu^-)^{[4.0, 6.0]}$	4.8791×10^{-8}	2.4 σ	3.2 σ
8	$\langle \frac{d\text{BR}}{dq^2} \rangle (B_s \rightarrow \phi \mu^+ \mu^-)^{[1.1, 2.5]}$	4.9961×10^{-8}	2.6 σ	3.2 σ
9	$\text{BR}(B^+ \rightarrow K^+ \nu \bar{\nu})$	9.7026×10^{-6}	1.4 σ	3.1 σ
10	$\langle \text{BR} \rangle (D^0 \rightarrow \pi^- e^+ \nu_e)^{[2.6, 2.98]}$	2.0647×10^{-5}	3 σ	3 σ
11	$\langle \frac{dR}{d\theta} \rangle (e^+ e^- \rightarrow W^+ W^-)^{[198.38, 0.8, 1.0]}$	7.236	3 σ	3 σ
12	$\langle P'_5 \rangle (B^0 \rightarrow K^{*0} \mu^+ \mu^-)^{[4, 6]}$	-0.64106	1.9 σ	2.7 σ
13	$\langle \text{BR} \rangle (D^0 \rightarrow K^- e^+ \nu_e)^{[1.6, 1.7]}$	0.00027193	2.6 σ	2.6 σ
14	$\text{BR}(W^\pm \rightarrow \tau^\pm \nu)$	0.10838	2.6 σ	2.6 σ
15	ϵ'/ϵ	-2.4761×10^{-5}	2.5 σ	2.6 σ
16	$\langle \frac{d\text{BR}}{dq^2} \rangle (B_s \rightarrow \phi \mu^+ \mu^-)^{[0.1, 0.98]}$	1.1062×10^{-7}	2.3 σ	2.5 σ
17	$A_{\text{FB}}^{0,b}$	0.10307	2.4 σ	2.4 σ
18	$\frac{\langle \text{BR} \rangle}{\text{BR}} (B \rightarrow D^* \tau^+ \nu)^{[10.4, 10.93]}$	0.018535	2.3 σ	2.3 σ
19	$\langle D_{A_{\text{FB}}}^{\mu e} \rangle (B^0 \rightarrow D^{*-} \ell^+ \nu)^{[0, 4.85]}$	-0.00085821	2.3 σ	2.3 σ
20	$\tilde{B}_n^{[0.591]}$	0.98894	2.3 σ	2.3 σ
21	$\langle \text{BR} \rangle (D^+ \rightarrow \pi^0 e^+ \nu_e)^{[2, 2.98]}$	0.00030592	2.3 σ	2.3 σ
22	A_e	0.14703	2.2 σ	2.2 σ
23	$\langle \frac{dR}{d\theta} \rangle (e^+ e^- \rightarrow W^+ W^-)^{[189.09, 0.8, 1.0]}$	6.253	2.2 σ	2.2 σ
24	$\langle \frac{d\text{BR}}{dq^2} \rangle (B^+ \rightarrow K^{*+} \mu^+ \mu^-)^{[15.0, 19.0]}$	5.5496×10^{-8}	1.4 σ	2.2 σ
25	$\langle \text{BR} \rangle (D^0 \rightarrow K^- e^+ \nu_e)^{[1.6, 1.88]}$	0.00041167	2.2 σ	2.2 σ
26	$\langle \frac{d\text{BR}}{dq^2} \rangle (B^+ \rightarrow K^{*+} \mu^+ \mu^-)^{[4.0, 6.0]}$	4.8167×10^{-8}	1.7 σ	2.2 σ
27	$\langle \frac{d\text{BR}}{dq^2} \rangle (B^\pm \rightarrow K^\pm \mu^+ \mu^-)^{[1.1, 2.0]}$	3.0582×10^{-8}	1.5 σ	2.2 σ
28	$\langle P'_4 \rangle (B^0 \rightarrow K^{*0} \mu^+ \mu^-)^{[4, 6]}$	-0.49222	2.1 σ	2.2 σ
29	$\langle P_3 \rangle (B^0 \rightarrow K^{*0} \mu^+ \mu^-)^{[1.1, 2.5]}$	0.0030283	2.2 σ	2.2 σ
30	$\langle S_7 \rangle (B_s \rightarrow \phi \mu^+ \mu^-)^{[0.1, 0.98]}$	-0.023453	2.1 σ	2.1 σ
31	$\langle P'_8 \rangle (B^0 \rightarrow K^{*0} \mu^+ \mu^-)^{[1.1, 2.5]}$	-0.013061	2.2 σ	2.1 σ
32	$\langle P_1 \rangle (B^0 \rightarrow K^{*0} \mu^+ \mu^-)^{[1.1, 2.5]}$	0.023738	2.1 σ	2.1 σ
33	$\frac{\langle \text{BR} \rangle}{\text{BR}} (B \rightarrow D^* \tau^+ \nu)^{[5.07, 5.6]}$	0.063081	2.1 σ	2.1 σ
34	$\langle \text{BR} \rangle (D^0 \rightarrow \pi^- e^+ \nu_e)^{[1.6, 1.8]}$	0.00015845	2.1 σ	2.1 σ
35	$\text{BR}(K_L \rightarrow e^+ e^-)$	1.9036×10^{-13}	2.1 σ	2.1 σ

	Observable	NP prediction	NP pull	SM pull
36	$\langle \frac{d\text{BR}}{dq^2} \rangle (B^0 \rightarrow K^{*0} \mu^+ \mu^-)^{[15.0, 19.0]}$	5.1507×10^{-8}	1.1σ	2.1σ
37	$\langle \bar{S}_3 \rangle (B_s \rightarrow \phi \mu^+ \mu^-)^{[4.0, 6.0]}$	-0.019113	2.1σ	2.1σ
38	$\text{BR}(B^\pm \rightarrow K^\pm \tau^+ \tau^-)$	4.3294×10^{-5}	2σ	2σ
39	$\text{BR}(\tau^- \rightarrow \mu^- \nu \bar{\nu})$	0.17281	2.2σ	2σ
40	$\langle P'_5 \rangle (B^+ \rightarrow K^{*+} \mu^+ \mu^-)^{[15, 19]}$	-0.5708	1.9σ	2σ
41	m_W	80.355	2σ	2σ
42	a_e	0.0011597	2σ	2σ
43	$\langle A_{\text{FB}}^{\ell h} \rangle (\Lambda_b \rightarrow \Lambda \mu^+ \mu^-)^{[15, 20]}$	0.15725	2.2σ	2σ
44	$\langle \text{BR} \rangle (D^0 \rightarrow K^- e^+ \nu_e)^{[1.5, 1.6]}$	0.00045096	2σ	2σ
45	$\langle P_2 \rangle (B^+ \rightarrow K^{*+} \mu^+ \mu^-)^{[4, 6]}$	0.18515	1.5σ	2σ
46	$\langle \bar{S}_7 \rangle (B_s \rightarrow \phi \mu^+ \mu^-)^{[4.0, 6.0]}$	-0.016215	2σ	2σ
47	$\text{BR}(D^+ \rightarrow \mu^+ \nu_\mu)$	0.00040895	2σ	2σ
48	$\langle \frac{d\text{BR}}{dq^2} \rangle (B_s \rightarrow \phi \mu^+ \mu^-)^{[1.0, 6.0]}$	4.8522×10^{-8}	1.6σ	2σ
49	$\langle \bar{S}_4 \rangle (B_s \rightarrow \phi \mu^+ \mu^-)^{[15.0, 18.9]}$	-0.30245	2σ	2σ
50	$\langle P_3 \rangle (B^+ \rightarrow K^{*+} \mu^+ \mu^-)^{[0.1, 0.98]}$	0.0013873	2σ	2σ
51	$\langle \frac{d\text{BR}}{dq^2} \rangle (B^\pm \rightarrow K^\pm \mu^+ \mu^-)^{[16.0, 17.0]}$	1.8595×10^{-8}	0.94σ	1.9σ
52	$\langle P_1 \rangle (B^0 \rightarrow K^{*0} \mu^+ \mu^-)^{[4.3, 6]}$	-0.16933	1.9σ	1.9σ
53	$\frac{\langle \text{BR} \rangle}{\text{BR}} (B \rightarrow D \tau^+ \nu)^{[7.73, 8.27]}$	0.091526	1.9σ	1.9σ
54	$\frac{\langle \text{BR} \rangle}{\text{BR}} (B \rightarrow D^* \tau^+ \nu)^{[7.2, 7.73]}$	0.10189	1.9σ	1.9σ
55	$\langle \frac{d\text{BR}}{dq^2} \rangle (B^0 \rightarrow K^0 \mu^+ \mu^-)^{[15.0, 22.0]}$	1.2027×10^{-8}	1.1σ	1.9σ
56	$\langle P'_5 \rangle (B^0 \rightarrow K^{*0} \mu^+ \mu^-)^{[2.5, 4]}$	-0.32641	0.94σ	1.9σ
57	$\langle \frac{d\text{BR}}{dq^2} \rangle (B^0 \rightarrow K^0 \mu^+ \mu^-)^{[4.0, 6.0]}$	2.7779×10^{-8}	1.3σ	1.9σ
58	$\langle \frac{dR}{d\theta} \rangle (e^+ e^- \rightarrow W^+ W^-)^{[198.38, -0.6, -0.4]}$	0.835	1.9σ	1.9σ
59	$\mu_{Zh}(h \rightarrow c\bar{c})$	1	1.8σ	1.8σ
60	$\langle \frac{d\text{BR}}{dq^2} \rangle (B^\pm \rightarrow K^\pm \mu^+ \mu^-)^{[4.0, 5.0]}$	3.0084×10^{-8}	1.1σ	1.8σ
61	$\langle \frac{d\text{BR}}{dq^2} \rangle (B^0 \rightarrow K^{*0} \mu^+ \mu^-)^{[4.0, 6.0]}$	4.4249×10^{-8}	1.1σ	1.8σ
62	$\overline{\text{BR}}(B_s \rightarrow \mu^+ \mu^-)$	3.6522×10^{-9}	1.8σ	1.8σ
63	$\langle \frac{d\text{BR}}{dq^2} \rangle (B^0 \rightarrow K^{*0} \mu^+ \mu^-)^{[4.3, 6]}$	4.4682×10^{-8}	1.2σ	1.8σ
64	$\langle \frac{dR}{d\theta} \rangle (e^+ e^- \rightarrow W^+ W^-)^{[198.38, 0.6, 0.8]}$	4.428	1.8σ	1.8σ
65	$\langle \frac{dR}{d\theta} \rangle (e^+ e^- \rightarrow W^+ W^-)^{[182.66, -1.0, -0.8]}$	0.702	1.8σ	1.8σ
66	$\langle \frac{d\text{BR}}{dq^2} \rangle (\Lambda_b \rightarrow \Lambda \mu^+ \mu^-)^{[15, 20]}$	6.168×10^{-8}	2.1σ	1.8σ
67	$R_{\tau\mu}(B \rightarrow D^* \ell^+ \nu)$	0.28997	0.77σ	1.7σ
68	$\langle P_2 \rangle (B^0 \rightarrow K^{*0} \mu^+ \mu^-)^{[4, 6]}$	0.18314	0.78σ	1.7σ
69	$\langle \frac{dR}{d\theta} \rangle (e^+ e^- \rightarrow W^+ W^-)^{[198.38, -1.0, -0.8]}$	0.542	1.7σ	1.7σ
70	$\langle \frac{d\text{BR}}{dq^2} \rangle (B^0 \rightarrow K^{*0} \mu^+ \mu^-)^{[1.1, 2.5]}$	4.2895×10^{-8}	1.3σ	1.7σ
71	$\langle \frac{dR}{d\theta} \rangle (e^+ e^- \rightarrow W^+ W^-)^{[182.66, 0.0, 0.2]}$	1.731	1.7σ	1.7σ
72	$\mu_{Wh}(h \rightarrow \tau^+ \tau^-)$	1	1.7σ	1.7σ
73	$\langle \frac{d\text{BR}}{dq^2} \rangle (B^\pm \rightarrow K^\pm \mu^+ \mu^-)^{[7.0, 8.0]}$	2.928×10^{-8}	0.99σ	1.7σ
74	$\langle \frac{dR}{d\theta} \rangle (e^+ e^- \rightarrow W^+ W^-)^{[205.92, 0.2, 0.4]}$	2.056	1.7σ	1.7σ
75	$\langle \frac{dR}{d\theta} \rangle (e^+ e^- \rightarrow W^+ W^-)^{[205.92, -0.6, -0.4]}$	0.77	1.7σ	1.7σ
76	$\langle \frac{d\text{BR}}{dq^2} \rangle (B^0 \rightarrow K^0 \mu^+ \mu^-)^{[2.0, 4.0]}$	2.8144×10^{-8}	1.2σ	1.7σ
77	$\langle \frac{d\text{BR}}{dq^2} \rangle (B^\pm \rightarrow K^\pm \mu^+ \mu^-)^{[5.0, 6.0]}$	2.9854×10^{-8}	0.98σ	1.7σ
78	$\langle \frac{d\text{BR}}{dq^2} \rangle (B^\pm \rightarrow K^\pm \mu^+ \mu^-)^{[14.82, 16.0]}$	2.0866×10^{-8}	0.78σ	1.7σ
79	$\mu_{t\bar{t}h}(h \rightarrow W^+ W^-)$	1	1.7σ	1.7σ
80	$\langle D_{A_{\text{FB}}}^{\mu e} \rangle (B^0 \rightarrow D^* \ell^+ \nu)^{[4.85, 10.689]}$	-0.00031982	1.7σ	1.7σ
81	$A_{\Delta\Gamma}(B_s \rightarrow \phi \gamma)$	0.030515	1.7σ	1.7σ
82	$\langle P'_5 \rangle (B^0 \rightarrow K^{*0} \mu^+ \mu^-)^{[0.1, 0.98]}$	0.72649	2σ	1.6σ
83	$R(e^+ e^- \rightarrow W^+ W^-)^{[182.7]}$	1	1.6σ	1.6σ

	Observable	NP prediction	NP pull	SM pull
84	$\langle \text{BR} \rangle(D^0 \rightarrow \pi^- e^+ \nu_e)^{[1.8, 2.0]}$	0.00012787	1.6 σ	1.6 σ
85	$\langle \text{BR} \rangle(D^0 \rightarrow \pi^- e^+ \nu_e)^{[2.0, 2.2]}$	9.7174×10^{-5}	1.6 σ	1.6 σ
86	$\frac{\langle \text{BR} \rangle}{\text{BR}}(B \rightarrow D\tau^+\nu)^{[9.0, 9.5]}$	0.066851	1.6 σ	1.6 σ
87	$\langle \frac{d\text{BR}}{dq^2} \rangle(B^\pm \rightarrow K^\pm \mu^+ \mu^-)^{[15.0, 22.0]}$	1.3064×10^{-8}	0.53 σ	1.6 σ
88	$\langle P'_6 \rangle(B^+ \rightarrow K^{*+} \mu^+ \mu^-)^{[15, 19]}$	-0.0025333	1.6 σ	1.6 σ
89	$\langle P'_6 \rangle(B^0 \rightarrow K^{*0} \mu^+ \mu^-)^{[4, 6]}$	-0.033642	1.5 σ	1.6 σ
90	$\langle \text{BR} \rangle(D^0 \rightarrow K^- e^+ \nu_e)^{[1.4, 1.6]}$	0.0011002	1.5 σ	1.5 σ
91	$\langle D_{P'_5}^{\mu e} \rangle(B^0 \rightarrow K^{*0} \ell^+ \ell^-)^{[14.18, 19.0]}$	-0.00080723	1.5 σ	1.5 σ
92	$R_{\tau\ell}(B \rightarrow D\ell^+\nu)$	0.35131	0.51 σ	1.5 σ
93	$\langle \text{BR} \rangle(D^0 \rightarrow \pi^- e^+ \nu_e)^{[2.2, 2.4]}$	6.745×10^{-5}	1.5 σ	1.5 σ
94	$A_{\text{FB}}^{0,\tau}$	0.016225	1.5 σ	1.5 σ
95	$\langle \bar{F}_L \rangle(B_s \rightarrow \phi \mu^+ \mu^-)^{[0.1, 0.98]}$	0.30943	0.93 σ	1.5 σ
96	$\langle \frac{d\text{BR}}{dq^2} \rangle(B^0 \rightarrow K^{*0} \mu^+ \mu^-)^{[2.5, 4.0]}$	4.0215×10^{-8}	0.93 σ	1.5 σ
97	$\langle \text{BR} \rangle(D^+ \rightarrow \pi^0 e^+ \nu_e)^{[1.2, 1.5]}$	0.00040451	1.5 σ	1.5 σ
98	$\langle \frac{d\text{BR}}{dq^2} \rangle(B^\pm \rightarrow K^\pm \mu^+ \mu^-)^{[6.0, 7.0]}$	2.9586×10^{-8}	0.78 σ	1.5 σ
99	$\tau_{B_s \rightarrow \mu\mu}$	2.4687×10^{12}	1.5 σ	1.5 σ
100	$\langle \bar{F}_L \rangle(B_s \rightarrow \phi \mu^+ \mu^-)^{[1.1, 4.0]}$	0.7804	0.98 σ	1.5 σ
101	$\langle \text{BR} \rangle(D^0 \rightarrow \pi^- e^+ \nu_e)^{[0.8, 1.0]}$	0.00026749	1.5 σ	1.5 σ
102	R_μ^0	20.735	1.5 σ	1.5 σ
103	$\langle R_{\mu e} \rangle(B^0 \rightarrow K^0 \ell^+ \ell^-)^{[1.1, 6.0]}$	1.0009	1.5 σ	1.5 σ
104	$\langle F_L \rangle(B^0 \rightarrow K^{*0} \mu^+ \mu^-)^{[1.1, 2.5]}$	0.71533	0.85 σ	1.5 σ
105	$\langle \frac{d\text{BR}}{dq^2} \rangle(B^\pm \rightarrow K^\pm \mu^+ \mu^-)^{[3.0, 4.0]}$	3.0276×10^{-8}	0.76 σ	1.5 σ
106	$\langle P'_5 \rangle(B^0 \rightarrow K^{*0} \mu^+ \mu^-)^{[1.1, 2.5]}$	0.275	0.59 σ	1.5 σ
107	$\text{BR}(B^- \rightarrow \pi^- \tau^+ e^-)$	0	1.5 σ	1.5 σ
108	$\langle \frac{dR}{d\theta} \rangle(e^+ e^- \rightarrow W^+ W^-)^{[182.66, 0.2, 0.4]}$	2.189	1.5 σ	1.5 σ
109	$F_L(B^0 \rightarrow D^{*-} \tau^+ \nu_\tau)$	0.46989	1.5 σ	1.5 σ
110	$\text{BR}(K_L \rightarrow \pi^+ e^+ \nu)$	0.41114	1.4 σ	1.4 σ
111	$\langle \frac{d\text{BR}}{dq^2} \rangle(B_s \rightarrow \phi \mu^+ \mu^-)^{[15.0, 19.0]}$	4.8663×10^{-8}	0.36 σ	1.4 σ
112	$\langle \bar{S}_4 \rangle(B_s \rightarrow \phi \mu^+ \mu^-)^{[0.1, 0.98]}$	0.078546	1.7 σ	1.4 σ
113	$\langle \text{BR} \rangle(B \rightarrow X_s e^+ e^-)^{[14.2, 25.0]}$	2.6875×10^{-7}	1.6 σ	1.4 σ
114	$\text{BR}(K_S \rightarrow \mu^+ \mu^-)$	5.1483×10^{-12}	1.4 σ	1.4 σ
115	$\langle R_{\mu e} \rangle(B^+ \rightarrow K^{*+} \ell^+ \ell^-)^{[0.045, 6.0]}$	0.97675	1.4 σ	1.4 σ
116	$\frac{\langle \text{BR} \rangle}{\text{BR}}(B \rightarrow D^* \tau^+ \nu)^{[6.0, 6.5]}$	0.080347	1.4 σ	1.4 σ
117	$\text{BR}(W^\pm \rightarrow \mu^\pm \nu)$	0.10842	1.4 σ	1.4 σ
118	$\langle A_9 \rangle(B^0 \rightarrow K^{*0} \mu^+ \mu^-)^{[15, 19]}$	4.2525×10^{-5}	1.4 σ	1.4 σ
119	$\langle \text{BR} \rangle(D^0 \rightarrow K^- e^+ \nu_e)^{[1.2, 1.4]}$	0.0019459	1.4 σ	1.4 σ
120	R_e^0	20.735	1.4 σ	1.4 σ
121	$R_{e\mu}(K^+ \rightarrow \ell^+ \nu)$	2.4754×10^{-5}	1.4 σ	1.4 σ
122	$\langle D_{S_3}^{\mu e} \rangle(B^0 \rightarrow D^{*-} \ell^+ \nu)^{[0, 4.85]}$	0.00090739	1.4 σ	1.4 σ
123	$\langle P'_5 \rangle(B^+ \rightarrow K^{*+} \mu^+ \mu^-)^{[4, 6]}$	-0.64813	1.1 σ	1.4 σ
124	$\langle \text{BR} \rangle(D^0 \rightarrow K^- e^+ \nu_e)^{[0.0, 0.1]}$	0.0040673	1.3 σ	1.3 σ
125	$\langle \frac{dR}{d\theta} \rangle(e^+ e^- \rightarrow W^+ W^-)^{[189.09, -0.2, 0.0]}$	1.403	1.3 σ	1.3 σ
126	$\langle D_{P'_5}^{\mu e} \rangle(B^0 \rightarrow K^{*0} \ell^+ \ell^-)^{[1.0, 6.0]}$	-0.0058815	1.3 σ	1.3 σ
127	$\langle \frac{d\text{BR}}{dq^2} \rangle(B^\pm \rightarrow K^\pm \mu^+ \mu^-)^{[0, 2]}$	3.0627×10^{-8}	0.71 σ	1.3 σ
128	$R_{\tau\mu}(B_c \rightarrow J/\psi \ell^+ \nu)$	0.30608	1.1 σ	1.3 σ
129	$\text{BR}(D_s \rightarrow e^+ \nu_e)$	1.2846×10^{-7}	1.3 σ	1.3 σ
130	$S_{\phi\gamma}$	-0.00022387	1.3 σ	1.3 σ
131	$\frac{\langle \text{BR} \rangle}{\text{BR}}(B \rightarrow D^* \tau^+ \nu)^{[8.27, 8.8]}$	0.10323	1.3 σ	1.3 σ

	Observable	NP prediction	NP pull	SM pull
132	$\text{BR}(K_S \rightarrow e^+ e^-)$	1.6122×10^{-16}	1.3σ	1.3σ
133	$\text{BR}(D^+ \rightarrow e^+ \nu_e)$	9.6268×10^{-9}	1.3σ	1.3σ
134	$\text{BR}(B^0 \rightarrow \rho^0 \nu \bar{\nu})$	1.798×10^{-7}	1.3σ	1.3σ
135	$\langle P'_4 \rangle (B^0 \rightarrow K^{*0} \mu^+ \mu^-)^{[2, 4]}$	-0.32639	1.3σ	1.3σ
136	$\text{BR}(D^0 \rightarrow \pi^- e^+ \nu_e)$	0.0026991	1.3σ	1.3σ
137	$\text{BR}(B^- \rightarrow \pi^- e^+ \tau^-)$	0	1.3σ	1.3σ
138	$\langle P'_8 \rangle (B^0 \rightarrow K^{*0} \mu^+ \mu^-)^{[4, 6]}$	-0.01042	1.3σ	1.3σ
139	$\text{BR}(B^0 \rightarrow \mu^+ \mu^-)$	1.0104×10^{-10}	1.3σ	1.3σ
140	$\langle R_{\mu e} \rangle (B^0 \rightarrow K^0 \ell^+ \ell^-)^{[4.0, 8.12]}$	1.0011	1.3σ	1.3σ
141	$\text{BR}(K_L \rightarrow \pi^0 \nu \bar{\nu})$	2.8803×10^{-11}	1.3σ	1.3σ
142	$\text{BR}(B_s \rightarrow K^* \mu^+ \mu^-)$	4.3607×10^{-8}	1.3σ	1.3σ
143	$\langle \frac{dR}{d\theta} \rangle (e^+ e^- \rightarrow W^+ W^-)^{[205.92, 0.0, 0.2]}$	1.561	1.3σ	1.3σ
144	$\text{BR}(B^0 \rightarrow K^{*0} \nu \bar{\nu})$	2.1038×10^{-5}	2.3σ	1.3σ
145	$\mu_{t\bar{t}h}(h \rightarrow VV)$	1	1.3σ	1.3σ
146	$\langle D_{S_3}^{\mu e} \rangle (B^0 \rightarrow D^{*-} \ell^+ \nu)^{[0, 10.689]}$	0.00066789	1.3σ	1.3σ
147	$\langle P_3 \rangle (B^0 \rightarrow K^{*0} \mu^+ \mu^-)^{[0.1, 0.98]}$	0.0013254	1.3σ	1.3σ
148	$S_{\psi K_S}$	0.70668	0.37σ	1.2σ
149	$\text{BR}(K^+ \rightarrow \pi^0 e^+ \nu)$	0.051557	1.2σ	1.2σ
150	$\frac{\langle \text{BR} \rangle}{\text{BR}} (B \rightarrow D \tau^+ \nu)^{[9.86, 10.4]}$	0.052844	1.2σ	1.2σ
151	$\text{BR}(\tau^+ \rightarrow K^+ \bar{\nu})$	0.0071673	1.6σ	1.2σ
152	$\mu_{\text{VBF}}(h \rightarrow bb)$	0.99999	1.2σ	1.2σ
153	$\langle F_L \rangle (B^0 \rightarrow K^{*0} \mu^+ \mu^-)^{[2, 4]}$	0.76974	0.97σ	1.2σ
154	$\langle \frac{dR}{d\theta} \rangle (e^+ e^- \rightarrow W^+ W^-)^{[182.66, 0.6, 0.8]}$	3.806	1.2σ	1.2σ
155	$\frac{\langle \text{BR} \rangle}{\text{BR}} (B \rightarrow D^* \tau^+ \nu)^{[4.0, 4.5]}$	0.02646	1.2σ	1.2σ
156	$\langle \text{BR} \rangle (D^0 \rightarrow \pi^- e^+ \nu_e)^{[1.0, 1.2]}$	0.00024295	1.2σ	1.2σ
157	$\langle \frac{d\text{BR}}{dq^2} \rangle (B^0 \rightarrow K^{*0} \mu^+ \mu^-)^{[2, 4.3]}$	4.0421×10^{-8}	0.62σ	1.2σ
158	$\mu_{Zh}(h \rightarrow bb)$	1	1.1σ	1.1σ
159	$\langle F_L \rangle (B^+ \rightarrow K^{*+} \mu^+ \mu^-)^{[1.1, 2.5]}$	0.72483	0.92σ	1.1σ
160	$\langle \text{BR} \rangle (D^+ \rightarrow K^0 e^+ \nu_e)^{[0.0, 0.2]}$	0.019949	1.1σ	1.1σ
161	$\text{BR}(B^+ \rightarrow K^{*+} \nu \bar{\nu})$	2.2678×10^{-5}	0.14σ	1.1σ
162	$\langle R_{\mu e} \rangle (B^\pm \rightarrow K^\pm \ell^+ \ell^-)^{[1.1, 6.0]}$	1.0009	1.1σ	1.1σ
163	$\mu_{Zh}(h \rightarrow W^+ W^-)$	1	1.1σ	1.1σ
164	$\mathcal{F}t(^{46}\text{V})$	4.6665×10^{27}	1.1σ	1.1σ
165	a_τ	0.0011772	1.1σ	1.1σ
166	$\mu_{Wh}(h \rightarrow W^+ W^-)$	1	1.1σ	1.1σ
167	$\langle P'_4 \rangle (B^+ \rightarrow K^{*+} \mu^+ \mu^-)^{[15, 19]}$	-0.63507	1.1σ	1.1σ
168	$R_{\mu e}(W^\pm \rightarrow \ell^\pm \nu)$	1	1.1σ	1.1σ
169	$\langle P'_4 \rangle (B^+ \rightarrow K^{*+} \mu^+ \mu^-)^{[1.1, 2.5]}$	-0.066804	1.1σ	1.1σ
170	$\langle P_1 \rangle (B^0 \rightarrow K^{*0} \mu^+ \mu^-)^{[4, 6]}$	-0.1661	1σ	1.1σ
171	$\langle \text{BR} \rangle (D^0 \rightarrow K^- e^+ \nu_e)^{[1.4, 1.5]}$	0.00064926	1.1σ	1.1σ
172	$\langle R_{\mu e} \rangle (B^0 \rightarrow K^0 \ell^+ \ell^-)^{[1.0, 6.0]}$	1.0009	1.1σ	1.1σ
173	$\langle P'_6 \rangle (B^0 \rightarrow K^{*0} \mu^+ \mu^-)^{[1.1, 2.5]}$	-0.069737	1.1σ	1.1σ
174	$\langle P'_8 \rangle (B^+ \rightarrow K^{*+} \mu^+ \mu^-)^{[0.1, 0.98]}$	-0.0304	1.1σ	1.1σ
175	$\langle \text{BR} \rangle (B \rightarrow X_s \mu^+ \mu^-)^{[1.0, 6.0]}$	1.5076×10^{-6}	0.87σ	1.1σ
176	$\langle P'_5 \rangle (B^+ \rightarrow K^{*+} \mu^+ \mu^-)^{[1.1, 2.5]}$	0.2491	0.87σ	1.1σ
177	$\text{BR}(K^+ \rightarrow \pi^0 \mu^+ \nu)$	0.034039	1.1σ	1.1σ
178	$\langle \frac{dR}{d\theta} \rangle (e^+ e^- \rightarrow W^+ W^-)^{[182.66, -0.8, -0.6]}$	0.841	1.1σ	1.1σ
179	$\langle \text{BR} \rangle (D^+ \rightarrow \pi^0 e^+ \nu_e)^{[0.9, 1.2]}$	0.00047905	1σ	1σ
180	$\langle P_1 \rangle (B^0 \rightarrow K^{*0} \mu^+ \mu^-)^{[2, 4]}$	-0.075668	1.1σ	1σ

	Observable	NP prediction	NP pull	SM pull
181	$\mathcal{F}t(^{34}\text{Ar})$	4.6665×10^{27}	1σ	1σ
182	$\langle \text{BR} \rangle(D^0 \rightarrow K^- e^+ \nu_e)^{[1.3, 1.4]}$	0.00086155	1σ	1σ
183	$\mu_{t\bar{t}h}(h \rightarrow \gamma\gamma)$	1	1σ	1σ
184	$\mu_{gg}(h \rightarrow Z\gamma)$	1	1σ	1σ
185	$\langle P_3 \rangle(B^0 \rightarrow K^{*0} \mu^+ \mu^-)^{[15, 19]}$	-0.00050642	1σ	1σ
186	$\mathcal{F}t(^{38}\text{Ca})$	4.6665×10^{27}	1σ	1σ
187	$\text{BR}(K_S \rightarrow \pi^+ \mu^+ \nu)$	0.00047682	1σ	1σ
188	$\langle \frac{dR}{d\theta} \rangle(e^+ e^- \rightarrow W^+ W^-)^{[182.66, -0.6, -0.4]}$	1.011	1σ	1σ
189	$\mu_{Wh}(h \rightarrow \gamma\gamma)$	1	0.99σ	0.99σ
190	$\langle P_1 \rangle(B^+ \rightarrow K^{*+} \mu^+ \mu^-)^{[0.1, 0.98]}$	0.042965	0.99σ	0.99σ
191	$\langle P'_4 \rangle(B^0 \rightarrow K^{*0} \mu^+ \mu^-)^{[0.1, 0.98]}$	0.21065	0.63σ	0.98σ
192	$\langle P'_5 \rangle(B^0 \rightarrow K^{*0} \mu^+ \mu^-)^{[15, 19]}$	-0.57101	1.3σ	0.98σ
193	$\langle R_{\mu e} \rangle(B^\pm \rightarrow K^\pm \ell^+ \ell^-)^{[1.0, 6.0]}$	1.0009	0.98σ	0.98σ
194	$\langle \text{BR} \rangle(D^+ \rightarrow \pi^0 e^+ \nu_e)^{[1.5, 2]}$	0.00048979	0.97σ	0.97σ
195	$\langle D_{S_7}^{\mu e} \rangle(B^0 \rightarrow D^{*-} \ell^+ \nu)^{[0, 4.85]}$	0	0.96σ	0.96σ
196	$\langle S_7 \rangle(B_s \rightarrow \phi \mu^+ \mu^-)^{[1.1, 4.0]}$	-0.026716	0.93σ	0.96σ
197	$\frac{\langle \text{BR} \rangle}{\text{BR}}(B \rightarrow D^* \tau^+ \nu)^{[10.5, 11.0]}$	0.010005	0.96σ	0.96σ
198	$\langle \text{BR} \rangle(D^0 \rightarrow \pi^- e^+ \nu_e)^{[0.0, 0.2]}$	0.00034413	0.95σ	0.95σ
199	$\langle \text{BR} \rangle(D^0 \rightarrow \pi^- e^+ \nu_e)^{[0.0, 0.3]}$	0.00051036	0.95σ	0.95σ
200	$\langle \frac{d\text{BR}}{dq^2} \rangle(B^\pm \rightarrow K^\pm \mu^+ \mu^-)^{[18.0, 19.24]}$	1.3317×10^{-8}	1.8σ	0.95σ
201	$\langle \frac{dR}{d\theta} \rangle(e^+ e^- \rightarrow W^+ W^-)^{[189.09, -0.8, -0.6]}$	0.781	0.95σ	0.95σ
202	$\tilde{a}_n^{[0.695]}$	-0.09921	0.95σ	0.95σ
203	$A_{\text{CP}}(B \rightarrow X_{s+d}\gamma)$	0	0.95σ	0.95σ
204	$\mu_{\text{VBF}}(h \rightarrow W^+ W^-)$	0.99999	0.94σ	0.94σ
205	$\langle A_7 \rangle(B^0 \rightarrow K^{*0} \mu^+ \mu^-)^{[1.1, 6]}$	0.0024616	0.94σ	0.94σ
206	$\langle \frac{dR}{d\theta} \rangle(e^+ e^- \rightarrow W^+ W^-)^{[189.09, -0.6, -0.4]}$	0.928	0.94σ	0.94σ
207	$\frac{\langle \text{BR} \rangle}{\text{BR}}(B \rightarrow D^* \tau^+ \nu)^{[7.73, 8.27]}$	0.10628	0.94σ	0.94σ
208	$\langle P_1 \rangle(B^+ \rightarrow K^{*+} \mu^+ \mu^-)^{[4, 6]}$	-0.16632	0.95σ	0.94σ
209	$R(e^+ e^- \rightarrow W^+ W^-)^{[204.9]}$	1	0.94σ	0.94σ
210	$\text{BR}(D^+ \rightarrow \pi^0 e^+ \nu_e)$	0.0034745	0.93σ	0.93σ
211	$\langle \frac{d\text{BR}}{dq^2} \rangle(B^\pm \rightarrow K^\pm \mu^+ \mu^-)^{[17.0, 18.0]}$	1.6265×10^{-8}	1.9σ	0.93σ
212	$\text{BR}(K^+ \rightarrow \pi^+ \nu\bar{\nu})$	8.4048×10^{-11}	0.93σ	0.92σ
213	$R(e^+ e^- \rightarrow W^+ W^-)^{[188.6]}$	1	0.92σ	0.92σ
214	$\langle \text{BR} \rangle(B \rightarrow X_s \mu^+ \mu^-)^{[14.2, 25.0]}$	3.0887×10^{-7}	1σ	0.91σ
215	$\langle D_{P'_4}^{\mu e} \rangle(B^0 \rightarrow K^{*0} \ell^+ \ell^-)^{[1.0, 6.0]}$	-0.0026233	0.91σ	0.91σ
216	$\frac{\langle \text{BR} \rangle}{\text{BR}}(B \rightarrow D \tau^+ \nu)^{[10.93, 11.47]}$	0.023172	0.9σ	0.9σ
217	$\langle \text{BR} \rangle(D^0 \rightarrow K^- e^+ \nu_e)^{[0.0, 0.2]}$	0.0078781	0.9σ	0.9σ
218	$\langle \frac{dR}{d\theta} \rangle(e^+ e^- \rightarrow W^+ W^-)^{[205.92, -0.4, -0.2]}$	0.972	0.9σ	0.9σ
219	$\langle \frac{d\text{BR}}{dq^2} \rangle(B^\pm \rightarrow K^\pm \mu^+ \mu^-)^{[2.0, 3.0]}$	3.0441×10^{-8}	0.19σ	0.9σ
220	A_τ	0.14714	0.93σ	0.9σ
221	$\langle \text{BR} \rangle(D^0 \rightarrow \pi^- e^+ \nu_e)^{[2.4, 2.6]}$	4.0233×10^{-5}	0.9σ	0.9σ
222	$\langle P'_4 \rangle(B^+ \rightarrow K^{*+} \mu^+ \mu^-)^{[0.1, 0.98]}$	0.20547	0.82σ	0.9σ
223	$\mathcal{F}t(^{10}\text{C})$	4.6665×10^{27}	0.9σ	0.89σ
224	$\frac{\langle \text{BR} \rangle}{\text{BR}}(B \rightarrow D \tau^+ \nu)^{[6.67, 7.2]}$	0.0957	0.89σ	0.89σ
225	$\langle A_7 \rangle(B^0 \rightarrow K^{*0} \mu^+ \mu^-)^{[15, 19]}$	0.00010727	0.89σ	0.89σ
226	$\mu_{gg}(h \rightarrow \mu^+ \mu^-)$	1	0.89σ	0.89σ
227	$\mu_{Zh}(h \rightarrow \gamma\gamma)$	1	0.88σ	0.88σ
228	$\mu_{gg}(h \rightarrow ZZ)$	1	0.88σ	0.88σ

	Observable	NP prediction	NP pull	SM pull
229	$\langle \text{BR} \rangle(D^0 \rightarrow \pi^- e^+ \nu_e)^{[1.2, 1.4]}$	0.00021643	0.87σ	0.87σ
230	$\frac{\langle \text{BR} \rangle}{\text{BR}}(B \rightarrow D\tau^+\nu)^{[10.0, 10.5]}$	0.046211	0.87σ	0.87σ
231	$\langle \frac{dR}{d\theta} \rangle(e^+e^- \rightarrow W^+W^-)^{[198.38, 0.4, 0.6]}$	3.003	0.87σ	0.87σ
232	$\text{BR}(B^- \rightarrow K^- e^+ \tau^-)$	0	0.87σ	0.87σ
233	$\langle \frac{dR}{d\theta} \rangle(e^+e^- \rightarrow W^+W^-)^{[182.66, 0.4, 0.6]}$	2.822	0.87σ	0.87σ
234	$\langle \text{BR} \rangle(D^0 \rightarrow \pi^- e^+ \nu_e)^{[1.5, 2]}$	0.00037676	0.86σ	0.87σ
235	$\frac{\langle \text{BR} \rangle}{\text{BR}}(B \rightarrow D\tau^+\nu)^{[8.8, 9.33]}$	0.074315	0.86σ	0.86σ
236	$\mu_{Vh}(h \rightarrow b\bar{b})$	1	0.86σ	0.86σ
237	$\frac{\langle \text{BR} \rangle}{\text{BR}}(B \rightarrow D\tau^+\nu)^{[5.5, 6.0]}$	0.081064	0.86σ	0.86σ
238	ΔM_s	1.2375×10^{-11}	0.83σ	0.85σ
239	$\tilde{A}_n^{[0.586]}$	-0.11027	0.85σ	0.85σ
240	$\text{BR}(\tau^- \rightarrow e^- \nu\bar{\nu})$	0.17768	1σ	0.85σ
241	$\frac{\langle \text{BR} \rangle}{\text{BR}}(B \rightarrow D^*\tau^+\nu)^{[8.8, 9.33]}$	0.097951	0.85σ	0.85σ
242	$\frac{\langle \text{BR} \rangle}{\text{BR}}(B \rightarrow D^*\tau^+\nu)^{[5.5, 6.0]}$	0.069886	0.84σ	0.84σ
243	$\langle \text{BR} \rangle(D^+ \rightarrow K^0 e^+ \nu_e)^{[1.4, 1.6]}$	0.0028176	0.84σ	0.84σ
244	$\frac{\langle \text{BR} \rangle}{\text{BR}}(B \rightarrow D\tau^+\nu)^{[7.2, 7.73]}$	0.094207	0.84σ	0.84σ
245	$\langle \text{BR} \rangle(D^+ \rightarrow K^0 e^+ \nu_e)^{[0.2, 0.4]}$	0.017368	0.84σ	0.84σ
246	$\langle \frac{d\text{BR}}{dq^2} \rangle(B^\pm \rightarrow \pi^\pm \mu^+ \mu^-)^{[4, 6]}$	6.3007×10^{-10}	0.84σ	0.84σ
247	$\frac{\langle \text{BR} \rangle}{\text{BR}}(B \rightarrow D^*\tau^+\nu)^{[6.13, 6.67]}$	0.08967	0.83σ	0.83σ
248	$\langle \frac{d\text{BR}}{dq^2} \rangle(B^\pm \rightarrow \pi^\pm \mu^+ \mu^-)^{[15, 22]}$	6.3412×10^{-10}	0.84σ	0.83σ
249	$\langle F_L \rangle(B_s \rightarrow \phi \mu^+ \mu^-)^{[4.0, 6.0]}$	0.73714	0.62σ	0.83σ
250	$\frac{\langle \text{BR} \rangle}{\text{BR}}(B \rightarrow D\tau^+\nu)^{[9.5, 10.0]}$	0.057131	0.83σ	0.83σ
251	$\frac{\langle \text{BR} \rangle}{\text{BR}}(B \rightarrow D\tau^+\nu)^{[10.4, 10.93]}$	0.0384	0.83σ	0.83σ
252	$A_{\text{FB}}^{0,c}$	0.073607	0.83σ	0.83σ
253	$\langle A_8 \rangle(B^0 \rightarrow K^{*0} \mu^+ \mu^-)^{[1.1, 6]}$	0.00062907	0.82σ	0.83σ
254	$\langle \text{BR} \rangle(D^0 \rightarrow K^- e^+ \nu_e)^{[1.2, 1.3]}$	0.0010843	0.82σ	0.82σ
255	$\text{BR}(W^\pm \rightarrow e^\pm \nu)$	0.10842	0.82σ	0.82σ
256	$\langle F_L \rangle(B^0 \rightarrow K^{*0} \mu^+ \mu^-)^{[1, 2]}$	0.67643	0.41σ	0.82σ
257	$\tilde{A}_n^{[0.559]}$	-0.11027	0.82σ	0.82σ
258	$\frac{\langle \text{BR} \rangle}{\text{BR}}(B \rightarrow D\tau^+\nu)^{[6.13, 6.67]}$	0.095554	0.82σ	0.82σ
259	$\langle \frac{dR}{d\theta} \rangle(e^+e^- \rightarrow W^+W^-)^{[189.09, 0.4, 0.6]}$	2.946	0.81σ	0.81σ
260	$\langle S_3 \rangle(B_s \rightarrow \phi \mu^+ \mu^-)^{[15.0, 18.9]}$	-0.21041	0.81σ	0.81σ
261	$\text{BR}(K_L \rightarrow \pi^+ \mu^+ \nu)$	0.27234	0.81σ	0.81σ
262	$\langle A_9 \rangle(B^0 \rightarrow K^{*0} \mu^+ \mu^-)^{[1.1, 6]}$	7.932×10^{-5}	0.8σ	0.8σ
263	$\mu_{VBF}(h \rightarrow \tau^+\tau^-)$	0.99999	0.8σ	0.8σ
264	$\langle P'_6 \rangle(B^0 \rightarrow K^{*0} \mu^+ \mu^-)^{[15, 19]}$	-0.0025344	0.8σ	0.8σ
265	$\frac{\langle \text{BR} \rangle}{\text{BR}}(B \rightarrow D^*\tau^+\nu)^{[6.67, 7.2]}$	0.096417	0.8σ	0.8σ
266	$\langle P_1 \rangle(B^0 \rightarrow K^{*0} \mu^+ \mu^-)^{[2, 4.3]}$	-0.085964	0.84σ	0.79σ
267	$\frac{\langle \text{BR} \rangle}{\text{BR}}(B \rightarrow D\tau^+\nu)^{[6.0, 6.5]}$	0.087331	0.78σ	0.78σ
268	$\langle D_{S_5}^{\mu e} \rangle(B^0 \rightarrow D^{*-} \ell^+ \nu)^{[0, 4.85]}$	-0.00099349	0.78σ	0.78σ
269	$\langle P_3 \rangle(B^+ \rightarrow K^{*+} \mu^+ \mu^-)^{[2.5, 4]}$	0.0032725	0.78σ	0.78σ
270	$\langle P'_4 \rangle(B^+ \rightarrow K^{*+} \mu^+ \mu^-)^{[4, 6]}$	-0.49084	0.81σ	0.78σ
271	$\tau_n^{[0.655]}$	1.3795×10^{27}	0.77σ	0.77σ
272	$\langle A_{\text{FB}}^\ell \rangle(\Lambda_b \rightarrow \Lambda \mu^+ \mu^-)^{[15, 20]}$	-0.3391	1.1σ	0.77σ
273	$\langle \frac{dR}{d\theta} \rangle(e^+e^- \rightarrow W^+W^-)^{[189.09, -1.0, -0.8]}$	0.661	0.77σ	0.77σ
274	$\langle F_L \rangle(B^0 \rightarrow K^{*0} \mu^+ \mu^-)^{[0, 2]}$	0.34966	0.53σ	0.77σ
275	$\langle \frac{dR}{d\theta} \rangle(e^+e^- \rightarrow W^+W^-)^{[205.92, 0.8, 1.0]}$	7.783	0.77σ	0.77σ

	Observable	NP prediction	NP pull	SM pull
276	$R(e^+e^- \rightarrow W^+W^-)^{[199.5]}$	1	0.76σ	0.76σ
277	$\langle BR \rangle (D^+ \rightarrow K^0 e^+ \nu_e)^{[1.0, 1.2]}$	0.0072975	0.76σ	0.76σ
278	$\langle A_{FB} \rangle (B^0 \rightarrow K^{*0} \mu^+ \mu^-)^{[4.3, 6]}$	0.090817	0.5σ	0.76σ
279	$\langle BR \rangle (D^0 \rightarrow \pi^- e^+ \nu_e)^{[0.9, 1.2]}$	0.00037376	0.76σ	0.76σ
280	$\langle P_1 \rangle (B^0 \rightarrow K^{*0} \mu^+ \mu^-)^{[2.5, 4]}$	-0.095799	0.7σ	0.75σ
281	$\frac{\langle BR \rangle}{BR} (B \rightarrow D \tau^+ \nu)^{[7.5, 8.0]}$	0.086997	0.75σ	0.75σ
282	$\langle \frac{dR}{d\theta} \rangle (e^+e^- \rightarrow W^+W^-)^{[198.38, -0.4, -0.2]}$	1.021	0.75σ	0.75σ
283	$\langle BR \rangle (D^0 \rightarrow K^- e^+ \nu_e)^{[1.7, 1.88]}$	0.00013987	0.75σ	0.75σ
284	$\langle BR \rangle (D^0 \rightarrow K^- e^+ \nu_e)^{[0.3, 0.4]}$	0.0032993	0.74σ	0.74σ
285	$\langle P_1 \rangle (B^0 \rightarrow K^{*0} e^+ e^-)^{[0.000784, 0.257]}$	0.032187	0.75σ	0.74σ
286	$\langle \frac{dR}{d\theta} \rangle (e^+e^- \rightarrow W^+W^-)^{[205.92, 0.4, 0.6]}$	2.903	0.74σ	0.74σ
287	$\langle BR \rangle (D^+ \rightarrow \pi^0 e^+ \nu_e)^{[0.0, 0.3]}$	0.00064889	0.74σ	0.74σ
288	$\langle BR \rangle (D^+ \rightarrow \pi^0 e^+ \nu_e)^{[0.6, 0.9]}$	0.00054491	0.73σ	0.73σ
289	$\langle BR \rangle (D^0 \rightarrow K^- e^+ \nu_e)^{[0.1, 0.2]}$	0.0038109	0.73σ	0.73σ
290	$\mu_{VBF}(h \rightarrow \gamma\gamma)$	0.99999	0.72σ	0.72σ
291	$\langle P_2 \rangle (B^0 \rightarrow K^{*0} \mu^+ \mu^-)^{[2.5, 4]}$	-0.19068	0.0058σ	0.72σ
292	$\langle \frac{dR}{d\theta} \rangle (e^+e^- \rightarrow W^+W^-)^{[198.38, 0.2, 0.4]}$	2.161	0.71σ	0.71σ
293	$\langle D_{S_5}^{\mu e} \rangle (B^0 \rightarrow D^{*-} \ell^+ \nu)^{[0, 10.689]}$	-0.00062141	0.71σ	0.71σ
294	$\frac{BR(B^0 \rightarrow K^{*0}\gamma)}{BR(B_s \rightarrow \phi\gamma)}$	1.032	0.7σ	0.7σ
295	$\langle A_{FB} \rangle (B^0 \rightarrow K^{*0} \mu^+ \mu^-)^{[1, 2]}$	-0.18354	0.54σ	0.7σ
296	R_b^0	0.21583	0.7σ	0.7σ
297	$\langle \frac{dR}{d\theta} \rangle (e^+e^- \rightarrow W^+W^-)^{[189.09, 0.0, 0.2]}$	1.715	0.7σ	0.7σ
298	$\langle P_3 \rangle (B^+ \rightarrow K^{*+} \mu^+ \mu^-)^{[4, 6]}$	0.0022846	0.7σ	0.7σ
299	R_{uc}^0	0.17224	0.69σ	0.69σ
300	$\langle BR \rangle (D^0 \rightarrow K^- e^+ \nu_e)^{[0.2, 0.4]}$	0.0068542	0.69σ	0.69σ
301	$\langle P'_6 \rangle (B^0 \rightarrow K^{*0} \mu^+ \mu^-)^{[0.1, 0.98]}$	-0.057199	0.72σ	0.69σ
302	$A_{FB}^{0,e}$	0.016213	0.69σ	0.69σ
303	$\mu_{gg}(h \rightarrow b\bar{b})$	1	0.68σ	0.68σ
304	$\frac{\langle BR \rangle}{BR} (B \rightarrow D \tau^+ \nu)^{[8.5, 9.0]}$	0.075222	0.68σ	0.68σ
305	$BR(B^+ \rightarrow \pi^+ \nu \bar{\nu})$	1.1241×10^{-7}	0.68σ	0.68σ
306	$\langle P_2 \rangle (B^+ \rightarrow K^{*+} \mu^+ \mu^-)^{[0.1, 0.98]}$	-0.13384	0.67σ	0.68σ
307	$\frac{\langle BR \rangle}{BR} (B \rightarrow D^* \tau^+ \nu)^{[7.5, 8.0]}$	0.097743	0.68σ	0.68σ
308	$\frac{\langle BR \rangle}{BR} (B \rightarrow D \tau^+ \nu)^{[10.5, 11.0]}$	0.034072	0.68σ	0.68σ
309	$\langle \frac{dR}{d\theta} \rangle (e^+e^- \rightarrow W^+W^-)^{[189.09, 0.6, 0.8]}$	4.122	0.68σ	0.68σ
310	$BR(B^+ \rightarrow \rho^+ \nu \bar{\nu})$	3.8763×10^{-7}	0.68σ	0.68σ
311	$\langle BR \rangle (D^0 \rightarrow K^- e^+ \nu_e)^{[0.5, 0.6]}$	0.0027908	0.68σ	0.68σ
312	$\langle F_L \rangle (B^0 \rightarrow K^{*0} \mu^+ \mu^-)^{[4, 6]}$	0.69875	0.46σ	0.67σ
313	$\mu_{t\bar{t}h}(h \rightarrow ZZ)$	1	0.67σ	0.67σ
314	$\frac{\langle BR \rangle}{BR} (B \rightarrow D \tau^+ \nu)^{[4.0, 4.53]}$	0.039796	0.67σ	0.67σ
315	$\frac{\langle BR \rangle}{BR} (B \rightarrow D^* \tau^+ \nu)^{[10.0, 10.5]}$	0.05617	0.66σ	0.66σ
316	$\mathcal{F}t(^{22}\text{Mg})$	4.6665×10^{27}	0.66σ	0.66σ
317	$\langle P'_5 \rangle (B^0 \rightarrow K^{*0} \mu^+ \mu^-)^{[4.3, 6]}$	-0.65737	1.1σ	0.66σ
318	Γ_Z	2.4939	0.69σ	0.66σ
319	$\langle \frac{dR}{d\theta} \rangle (e^+e^- \rightarrow W^+W^-)^{[182.66, -0.2, 0.0]}$	1.402	0.65σ	0.65σ
320	$R_{\tau e}(W^\pm \rightarrow \ell^\pm \nu)$	0.99968	0.64σ	0.65σ
321	$\langle \frac{dR}{d\theta} \rangle (e^+e^- \rightarrow W^+W^-)^{[205.92, -1.0, -0.8]}$	0.532	0.64σ	0.64σ
322	$BR(B^0 \rightarrow \pi^0 \nu \bar{\nu})$	5.2284×10^{-8}	0.63σ	0.63σ
323	$\langle BR \rangle (D^+ \rightarrow K^0 e^+ \nu_e)^{[1.2, 1.4]}$	0.0049637	0.63σ	0.63σ

	Observable	NP prediction	NP pull	SM pull
324	$\langle \frac{d\text{BR}}{dq^2} \rangle (B^\pm \rightarrow K^\pm \mu^+ \mu^-)^{[0.1, 0.98]}$	3.0622×10^{-8}	0.079σ	0.63σ
325	$\langle F_L \rangle (B^0 \rightarrow K^{*0} \mu^+ \mu^-)^{[2.5, 4]}$	0.77043	0.23σ	0.63σ
326	$S_{K^*\gamma}$	-0.022736	0.64σ	0.63σ
327	$\frac{\langle \text{BR} \rangle}{\text{BR}} (B \rightarrow D\tau^+\nu)^{[4.0, 4.5]}$	0.036939	0.63σ	0.63σ
328	$\mu_{Wh}(h \rightarrow bb)$	1	0.62σ	0.62σ
329	$\langle A_{\text{FB}} \rangle (B^0 \rightarrow K^{*0} \mu^+ \mu^-)^{[2, 4.3]}$	-0.068851	0.3σ	0.62σ
330	$\langle P_3 \rangle (B^0 \rightarrow K^{*0} \mu^+ \mu^-)^{[4, 6]}$	0.0023076	0.62σ	0.62σ
331	$\langle F_L \rangle (B^0 \rightarrow K^{*0} \mu^+ \mu^-)^{[0.1, 0.98]}$	0.26349	0.13σ	0.62σ
332	$\langle \text{BR} \rangle (D^0 \rightarrow K^- e^+ \nu_e)^{[1.0, 1.1]}$	0.001552	0.62σ	0.62σ
333	$R_{\tau\mu}(W^\pm \rightarrow \ell^\pm \nu)$	0.99968	0.59σ	0.61σ
334	$R(e^+ e^- \rightarrow W^+ W^-)^{[195.5]}$	1	0.61σ	0.61σ
335	$\frac{\langle \text{BR} \rangle}{\text{BR}} (B \rightarrow D^* \tau^+ \nu)^{[4.53, 5.07]}$	0.047596	0.61σ	0.61σ
336	$\langle \frac{dR}{d\theta} \rangle (e^+ e^- \rightarrow W^+ W^-)^{[205.92, -0.8, -0.6]}$	0.642	0.61σ	0.61σ
337	$\mu_{Zh}(h \rightarrow \tau^+ \tau^-)$	1	0.6σ	0.6σ
338	$\text{BR}(B^0 \rightarrow \pi^- \tau^+ \nu_\tau)$	0.00010404	0.6σ	0.6σ
339	$\langle \text{BR} \rangle (D^0 \rightarrow \pi^- e^+ \nu_e)^{[0.6, 0.8]}$	0.00028991	0.6σ	0.59σ
340	$\langle P'_8 \rangle (B^+ \rightarrow K^{*+} \mu^+ \mu^-)^{[15, 19]}$	0.0007378	0.6σ	0.59σ
341	$\langle R_{\mu e} \rangle (B^+ \rightarrow K^{*+} \ell^+ \ell^-)^{[15.0, 19.0]}$	0.9978	0.59σ	0.59σ
342	$\mathcal{F}t(^{14}\text{O})$	4.6665×10^{27}	0.58σ	0.59σ
343	$\langle R_{\mu e} \rangle (B^\pm \rightarrow K^\pm \ell^+ \ell^-)^{[4.0, 8.12]}$	1.0011	0.59σ	0.59σ
344	A_b	0.93471	0.59σ	0.59σ
345	$\mu_{gg}(h \rightarrow W^+ W^-)$	1	0.58σ	0.58σ
346	$\langle F_L \rangle (B^0 \rightarrow K^{*0} \mu^+ \mu^-)^{[4.3, 6]}$	0.69169	0.48σ	0.58σ
347	$\lambda_{AB}^{[0.581]}$	-1.251	0.58σ	0.58σ
348	D_n	0	0.57σ	0.57σ
349	$\text{BR}(B^- \rightarrow K^- \tau^+ \mu^-)$	0	0.57σ	0.57σ
350	$\langle A_{\text{FB}} \rangle (B^0 \rightarrow K^{*0} \mu^+ \mu^-)^{[0, 2]}$	-0.11349	0.6σ	0.57σ
351	$\langle P'_6 \rangle (B^0 \rightarrow K^{*0} \mu^+ \mu^-)^{[2.5, 4]}$	-0.055059	0.55σ	0.57σ
352	$R_{\mu e}(B \rightarrow D^* \ell^+ \nu)$	0.99682	0.56σ	0.56σ
353	$\text{BR}(K_S \rightarrow \pi^+ e^+ \nu)$	0.00071984	0.56σ	0.56σ
354	$\mathcal{F}t(^{38m}\text{K})$	4.6665×10^{27}	0.57σ	0.56σ
355	$\frac{\langle \text{BR} \rangle}{\text{BR}} (B \rightarrow D\tau^+ \nu)^{[8.27, 8.8]}$	0.083047	0.56σ	0.56σ
356	$\overline{\text{BR}}(B_s \rightarrow e^+ e^-)$	8.5492×10^{-14}	0.55σ	0.55σ
357	$\langle P'_5 \rangle (B^+ \rightarrow K^{*+} \mu^+ \mu^-)^{[0.1, 0.98]}$	0.72305	0.68σ	0.55σ
358	$\frac{\langle \text{BR} \rangle}{\text{BR}} (B \rightarrow D\tau^+ \nu)^{[4.53, 5.07]}$	0.062198	0.53σ	0.53σ
359	$\langle R_{\mu e} \rangle (B^0 \rightarrow K^0 \ell^+ \ell^-)^{[14.18, 19.0]}$	1.0027	0.53σ	0.53σ
360	$\langle D_{S7}^{\mu e} \rangle (B^0 \rightarrow D^{*-} \ell^+ \nu)^{[0, 10.689]}$	0	0.53σ	0.53σ
361	$\langle P'_5 \rangle (B^0 \rightarrow K^{*0} \mu^+ \mu^-)^{[1, 2]}$	0.40401	0.87σ	0.53σ
362	$\langle \text{BR} \rangle (D^0 \rightarrow K^- e^+ \nu_e)^{[0.2, 0.3]}$	0.0035548	0.53σ	0.53σ
363	$\langle P_3 \rangle (B^+ \rightarrow K^{*+} \mu^+ \mu^-)^{[15, 19]}$	-0.00050629	0.53σ	0.53σ
364	$\langle \frac{d\text{BR}}{dq^2} \rangle (B^0 \rightarrow K^{*0} \mu^+ \mu^-)^{[0, 2]}$	7.9608×10^{-8}	0.66σ	0.53σ
365	$A_{\text{FB}}^{0,\mu}$	0.016213	0.53σ	0.53σ
366	$\langle A_8 \rangle (B^0 \rightarrow K^{*0} \mu^+ \mu^-)^{[15, 19]}$	5.5517×10^{-5}	0.52σ	0.52σ
367	$\langle P'_5 \rangle (B^0 \rightarrow K^{*0} \mu^+ \mu^-)^{[0.04, 2]}$	0.59068	0.27σ	0.52σ
368	$\langle P_1 \rangle (B^+ \rightarrow K^{*+} \mu^+ \mu^-)^{[1.1, 2.5]}$	0.022564	0.52σ	0.52σ
369	$\langle \text{BR} \rangle (D^0 \rightarrow \pi^- e^+ \nu_e)^{[1.4, 1.6]}$	0.00018815	0.52σ	0.52σ
370	$\frac{\langle \text{BR} \rangle}{\text{BR}} (B \rightarrow D\tau^+ \nu)^{[11.5, 12.0]}$	0.0019321	0.52σ	0.52σ
371	$\text{BR}(\pi^+ \rightarrow e^+ \nu)$	0.00012341	0.51σ	0.51σ
372	$\langle \text{BR} \rangle (D^0 \rightarrow \pi^- e^+ \nu_e)^{[0.3, 0.6]}$	0.00047214	0.51σ	0.51σ

	Observable	NP prediction	NP pull	SM pull
373	$\langle D_{A_{\text{FB}}}^{\mu e} \rangle (B^0 \rightarrow D^{*-} \ell^+ \nu)^{[0, 10.689]}$	-0.00052619	0.51 σ	0.51 σ
374	$\langle S_3 \rangle (B_s \rightarrow \phi \mu^+ \mu^-)^{[1.1, 4.0]}$	0.0017998	0.53 σ	0.51 σ
375	$\mathcal{F}t(^{26m}\text{Al})$	4.6665×10^{27}	0.51 σ	0.51 σ
376	$R(e^+ e^- \rightarrow W^+ W^-)^{[206.6]}$	1	0.5 σ	0.5 σ
377	$\langle R_{\mu e} \rangle (B^0 \rightarrow K^0 \ell^+ \ell^-)^{[0.1, 4.0]}$	1.0005	0.5 σ	0.5 σ
378	$\text{BR}(K_L \rightarrow \mu^+ \mu^-)$	7.368×10^{-9}	0.52 σ	0.5 σ
379	$\frac{\langle \text{BR} \rangle}{\text{BR}} (B \rightarrow D^* \tau^+ \nu)^{[4.5, 5.0]}$	0.042534	0.5 σ	0.5 σ
380	$\mu_{t\bar{t}h}(h \rightarrow \tau^+ \tau^-)$	1	0.49 σ	0.49 σ
381	$\langle \frac{dR}{d\theta} \rangle (e^+ e^- \rightarrow W^+ W^-)^{[182.66, -0.4, -0.2]}$	1.181	0.49 σ	0.49 σ
382	$\langle \frac{d\text{BR}}{dq^2} \rangle (B^+ \rightarrow K^{*+} \mu^+ \mu^-)^{[2.0, 4.0]}$	4.4008×10^{-8}	0.76 σ	0.49 σ
383	$\langle \frac{d\text{BR}}{dq^2} \rangle (B^0 \rightarrow K^0 \mu^+ \mu^-)^{[0, 2]}$	2.8395×10^{-8}	0.24 σ	0.49 σ
384	$\text{BR}(D^0 \rightarrow K^- \mu^+ \nu_\mu)$	0.035387	0.48 σ	0.48 σ
385	$\text{BR}(B^0 \rightarrow K^0 \nu \bar{\nu})$	8.9779×10^{-6}	0.022 σ	0.48 σ
386	$\langle P_2 \rangle (B^+ \rightarrow K^{*+} \mu^+ \mu^-)^{[1.1, 2.5]}$	-0.45787	0.5 σ	0.48 σ
387	$\text{BR}(B_c \rightarrow \tau^+ \nu)$	0.02813	0.55 σ	0.47 σ
388	$\langle F_L \rangle (B^+ \rightarrow K^{*+} \mu^+ \mu^-)^{[15, 19]}$	0.34002	0.47 σ	0.46 σ
389	$\langle \text{BR} \rangle (D^+ \rightarrow K^0 e^+ \nu_e)^{[1.6, 1.88]}$	0.0010683	0.46 σ	0.46 σ
390	$\langle \text{BR} \rangle (D^0 \rightarrow K^- e^+ \nu_e)^{[1.1, 1.2]}$	0.0013151	0.46 σ	0.46 σ
391	$\frac{\langle \text{BR} \rangle}{\text{BR}} (B \rightarrow D^* \tau^+ \nu)^{[7.0, 7.5]}$	0.094374	0.45 σ	0.45 σ
392	$\langle P'_4 \rangle (B^0 \rightarrow K^{*0} \mu^+ \mu^-)^{[0.04, 2]}$	0.1283	0.49 σ	0.45 σ
393	$\overline{\text{BR}}(B_s \rightarrow \phi \gamma)$	4.0482×10^{-5}	0.44 σ	0.45 σ
394	$\mathcal{F}t(^{74}\text{Rb})$	4.6665×10^{27}	0.45 σ	0.45 σ
395	$\langle D_{S_9}^{\mu e} \rangle (B^0 \rightarrow D^{*-} \ell^+ \nu)^{[4.85, 10.689]}$	0	0.45 σ	0.45 σ
396	A_s	0.93552	0.45 σ	0.45 σ
397	$\text{BR}(B^- \rightarrow K^{*-} e^+ \mu^-)$	0	0.45 σ	0.45 σ
398	$\langle \frac{dR}{d\theta} \rangle (e^+ e^- \rightarrow W^+ W^-)^{[198.38, -0.8, -0.6]}$	0.664	0.45 σ	0.45 σ
399	$\frac{\langle \text{BR} \rangle}{\text{BR}} (B \rightarrow D^* \tau^+ \nu)^{[9.86, 10.4]}$	0.067679	0.44 σ	0.44 σ
400	$\langle F_L \rangle (B^0 \rightarrow K^{*0} \mu^+ \mu^-)^{[0.04, 2]}$	0.34966	0.74 σ	0.44 σ
401	$\langle P_2 \rangle (B^0 \rightarrow K^{*0} \mu^+ \mu^-)^{[15, 19]}$	0.35667	0.063 σ	0.44 σ
402	$\langle \text{BR} \rangle (D^0 \rightarrow K^- e^+ \nu_e)^{[0.9, 1.0]}$	0.0017938	0.44 σ	0.44 σ
403	$\text{BR}(D^+ \rightarrow K^0 e^+ \nu_e)$	0.090179	0.44 σ	0.44 σ
404	$\langle P'_4 \rangle (B^+ \rightarrow K^{*+} \mu^+ \mu^-)^{[2.5, 4]}$	-0.36856	0.46 σ	0.44 σ
405	$\frac{\langle \text{BR} \rangle}{\text{BR}} (B \rightarrow D \tau^+ \nu)^{[11.0, 11.5]}$	0.019888	0.43 σ	0.43 σ
406	$\mu_{W h}(h \rightarrow ZZ)$	1	0.43 σ	0.43 σ
407	$\langle \text{BR} \rangle (B \rightarrow X_s e^+ e^-)^{[1.0, 6.0]}$	1.5637×10^{-6}	0.74 σ	0.42 σ
408	$\langle P_1 \rangle (B^0 \rightarrow K^{*0} \mu^+ \mu^-)^{[15, 19]}$	-0.62282	0.42 σ	0.42 σ
409	$\langle F_L \rangle (B^0 \rightarrow K^{*0} \mu^+ \mu^-)^{[2, 4.3]}$	0.76593	0.12 σ	0.42 σ
410	$\mu_{gg}(h \rightarrow \gamma\gamma)$	1	0.42 σ	0.42 σ
411	$\langle P_2 \rangle (B^0 \rightarrow K^{*0} e^+ e^-)^{[0.000784, 0.257]}$	-0.012119	0.42 σ	0.42 σ
412	a_n	-0.09921	0.42 σ	0.42 σ
413	$\langle \frac{dR}{d\theta} \rangle (e^+ e^- \rightarrow W^+ W^-)^{[189.09, -0.4, -0.2]}$	1.137	0.41 σ	0.41 σ
414	$\langle R_{\mu e} \rangle (B^0 \rightarrow K^{*0} \ell^+ \ell^-)^{[1.1, 6.0]}$	0.99609	0.41 σ	0.41 σ
415	$\langle \overline{S}_3 \rangle (B_s \rightarrow \phi \mu^+ \mu^-)^{[0.1, 0.98]}$	0.025706	0.42 σ	0.41 σ
416	$\langle \overline{F}_L \rangle (B_s \rightarrow \phi \mu^+ \mu^-)^{[15.0, 18.9]}$	0.34116	0.41 σ	0.4 σ
417	$\langle P_1 \rangle (B^0 \rightarrow K^{*0} \mu^+ \mu^-)^{[0.1, 0.98]}$	0.041961	0.42 σ	0.4 σ
418	$\langle D_{S_9}^{\mu e} \rangle (B^0 \rightarrow D^{*-} \ell^+ \nu)^{[0, 10.689]}$	0	0.4 σ	0.4 σ
419	$\langle D_{S_7}^{\mu e} \rangle (B^0 \rightarrow D^{*-} \ell^+ \nu)^{[4.85, 10.689]}$	0	0.39 σ	0.39 σ
420	$\text{BR}(D^+ \rightarrow \tau^+ \nu_\tau)$	0.0010903	0.4 σ	0.39 σ
421	$\mathcal{F}t(^{54}\text{Co})$	4.6665×10^{27}	0.39 σ	0.39 σ

	Observable	NP prediction	NP pull	SM pull
422	R_τ^0	20.779	0.33σ	0.38σ
423	$\langle \frac{dR}{d\theta} \rangle (e^+ e^- \rightarrow W^+ W^-)^{[198.38, 0.0, 0.2]}$	1.666	0.38σ	0.38σ
424	$\langle \text{BR} \rangle (D^0 \rightarrow \pi^- e^+ \nu_e)^{[0.4, 0.6]}$	0.00031016	0.38σ	0.38σ
425	$\langle \frac{d\text{BR}}{dq^2} \rangle (B^\pm \rightarrow K^\pm \mu^+ \mu^-)^{[2, 4.3]}$	3.0332×10^{-8}	0.16σ	0.38σ
426	$\langle D_{S_3}^{\mu e} \rangle (B^0 \rightarrow D^{*-} \ell^+ \nu)^{[4.85, 10.689]}$	0.00064878	0.37σ	0.37σ
427	$\langle R_{\mu e} \rangle (B^0 \rightarrow K^{*0} \ell^+ \ell^-)^{[0.1, 8.0]}$	0.99422	0.36σ	0.37σ
428	$\langle S_4 \rangle (B_s \rightarrow \phi \mu^+ \mu^-)^{[1.1, 4.0]}$	-0.082084	0.35σ	0.37σ
429	$\langle \frac{d\text{BR}}{dq^2} \rangle (B^0 \rightarrow K^0 \mu^+ \mu^-)^{[2, 4.3]}$	2.8119×10^{-8}	0.14σ	0.36σ
430	$\langle R_{\mu e} \rangle (B^0 \rightarrow K^{*0} \ell^+ \ell^-)^{[15.0, 19.0]}$	0.9978	0.36σ	0.36σ
431	$\langle \text{BR} \rangle (D^+ \rightarrow \pi^0 e^+ \nu_e)^{[0.3, 0.6]}$	0.00060153	0.35σ	0.35σ
432	$\mu_{\text{VBF}}(h \rightarrow ZZ)$	0.99999	0.35σ	0.35σ
433	$\langle P_1 \rangle (B^0 \rightarrow K^{*0} \mu^+ \mu^-)^{[0.04, 2]}$	0.040921	0.34σ	0.35σ
434	$ \epsilon_K $	0.0019381	1σ	0.34σ
435	$\langle A_{\text{FB}}^h \rangle (\Lambda_b \rightarrow \Lambda \mu^+ \mu^-)^{[15, 20]}$	-0.3183	0.34σ	0.34σ
436	$\langle \text{BR} \rangle (D^+ \rightarrow K^0 e^+ \nu_e)^{[0.4, 0.6]}$	0.014798	0.34σ	0.34σ
437	$\langle P_2 \rangle (B^+ \rightarrow K^{*+} \mu^+ \mu^-)^{[15, 19]}$	0.35656	0.16σ	0.34σ
438	A_μ	0.14703	0.34σ	0.34σ
439	$\overline{\text{BR}}(B_s \rightarrow \tau^+ \tau^-)$	0.00020065	0.4σ	0.33σ
440	$\text{BR}(\tau^- \rightarrow e^- \mu^+ e^-)$	0	0.32σ	0.32σ
441	$\mu_{t\bar{t}h}(h \rightarrow bb)$	1	0.32σ	0.32σ
442	$\text{BR}(D^+ \rightarrow K^0 \mu^+ \nu_\mu)$	0.089837	0.32σ	0.32σ
443	$\frac{\langle \text{BR} \rangle}{\text{BR}}(B \rightarrow D \tau^+ \nu)^{[6.5, 7.0]}$	0.090071	0.32σ	0.32σ
444	$\langle P'_8 \rangle (B^0 \rightarrow K^{*0} \mu^+ \mu^-)^{[2.5, 4]}$	-0.014458	0.29σ	0.31σ
445	$\langle F_L \rangle (B^+ \rightarrow K^{*+} \mu^+ \mu^-)^{[4, 6]}$	0.70129	0.21σ	0.31σ
446	$\langle \text{BR} \rangle (D^0 \rightarrow K^- e^+ \nu_e)^{[0.4, 0.6]}$	0.0058353	0.31σ	0.31σ
447	$\frac{\langle \text{BR} \rangle}{\text{BR}}(B \rightarrow D \tau^+ \nu)^{[4.5, 5.0]}$	0.05594	0.3σ	0.3σ
448	R_n	0	0.3σ	0.3σ
449	$\text{BR}(\bar{B}^0 \rightarrow \bar{K}^{*0} \mu^+ e^-)$	0	0.3σ	0.3σ
450	$\langle R_{\mu e} \rangle (B^\pm \rightarrow K^\pm \ell^+ \ell^-)^{[14.18, 19.0]}$	1.0027	0.29σ	0.29σ
451	σ_{had}^0	0.00010655	0.4σ	0.29σ
452	$\langle F_L \rangle (B^+ \rightarrow K^{*+} \mu^+ \mu^-)^{[0.1, 0.98]}$	0.27359	0.51σ	0.29σ
453	$\langle P_2 \rangle (B^+ \rightarrow K^{*+} \mu^+ \mu^-)^{[2.5, 4]}$	-0.18323	0.7σ	0.28σ
454	$\langle P'_5 \rangle (B^+ \rightarrow K^{*+} \mu^+ \mu^-)^{[2.5, 4]}$	-0.34555	0.42σ	0.28σ
455	$\langle R_{\mu e} \rangle (B^\pm \rightarrow K^\pm \ell^+ \ell^-)^{[0.1, 4.0]}$	1.0005	0.28σ	0.28σ
456	$\langle P'_8 \rangle (B^+ \rightarrow K^{*+} \mu^+ \mu^-)^{[4, 6]}$	-0.010386	0.29σ	0.28σ
457	$\langle D_{S_9}^{\mu e} \rangle (B^0 \rightarrow D^{*-} \ell^+ \nu)^{[0, 4.85]}$	0	0.28σ	0.28σ
458	$\langle \text{BR} \rangle (D^0 \rightarrow \pi^- e^+ \nu_e)^{[1.2, 1.5]}$	0.00031414	0.27σ	0.27σ
459	$\langle P'_5 \rangle (B^0 \rightarrow K^{*0} \mu^+ \mu^-)^{[2, 4.3]}$	-0.27698	0.72σ	0.27σ
460	$S_{\psi\phi}$	0.036815	0.13σ	0.26σ
461	$\langle D_{S_5}^{\mu e} \rangle (B^0 \rightarrow D^{*-} \ell^+ \nu)^{[4.85, 10.689]}$	-0.00041299	0.26σ	0.26σ
462	$\langle P_3 \rangle (B^0 \rightarrow K^{*0} \mu^+ \mu^-)^{[2.5, 4]}$	0.0032846	0.26σ	0.25σ
463	$R(W^+ \rightarrow cX)$	0.50001	0.25σ	0.25σ
464	$x_{12}^{\text{Im}, D}$	-2.0104×10^{-18}	0.25σ	0.25σ
465	$\langle P'_5 \rangle (B^0 \rightarrow K^{*0} \mu^+ \mu^-)^{[2, 4]}$	-0.23357	0.24σ	0.25σ
466	$\text{BR}(B^- \rightarrow K^{*-} \mu^+ e^-)$	0	0.25σ	0.25σ
467	$\langle P'_4 \rangle (B^0 \rightarrow K^{*0} \mu^+ \mu^-)^{[2.5, 4]}$	-0.36988	0.37σ	0.25σ
468	$\mu_{\text{VBF}}(h \rightarrow \mu^+ \mu^-)$	0.99999	0.24σ	0.24σ
469	$\mu_{Zh}(h \rightarrow ZZ)$	1	0.23σ	0.23σ
470	$\langle P'_6 \rangle (B^+ \rightarrow K^{*+} \mu^+ \mu^-)^{[1.1, 2.5]}$	-0.054293	0.23σ	0.23σ

	Observable	NP prediction	NP pull	SM pull
471	$\langle \frac{d\text{BR}}{dq^2} \rangle (B^+ \rightarrow K^{*+} \mu^+ \mu^-)^{[0, 2]}$	8.3592×10^{-8}	0.17σ	0.23σ
472	$\Gamma(\pi^+ \rightarrow \mu^+ \nu)$	2.5202×10^{-17}	0.23σ	0.23σ
473	$\mathcal{F}t(^{50}\text{Mn})$	4.6665×10^{27}	0.23σ	0.23σ
474	$\mu_{Vh}(h \rightarrow ZZ)$	1	0.23σ	0.23σ
475	$\text{BR}(B^0 \rightarrow e^+ e^-)$	2.3651×10^{-15}	0.22σ	0.22σ
476	$\frac{\langle \text{BR} \rangle}{\text{BR}} (B \rightarrow D^* \tau^+ \nu)^{[5.6, 6.13]}$	0.076828	0.22σ	0.22σ
477	$\frac{\langle \text{BR} \rangle}{\text{BR}} (B \rightarrow D \tau^+ \nu)^{[11.47, 12.0]}$	0.0025446	0.22σ	0.22σ
478	$\text{BR}(B^\pm \rightarrow \pi^\pm e^+ e^-)$	1.5845×10^{-8}	0.21σ	0.22σ
479	$R(e^+ e^- \rightarrow W^+ W^-)^{[191.6]}$	1	0.21σ	0.21σ
480	$\langle P'_8 \rangle (B^+ \rightarrow K^{*+} \mu^+ \mu^-)^{[1.1, 2.5]}$	-0.023263	0.21σ	0.21σ
481	$\langle F_L \rangle (B^0 \rightarrow K^{*0} e^+ e^-)^{[0.000784, 0.257]}$	0.044367	0.018σ	0.21σ
482	$\frac{\langle \text{BR} \rangle}{\text{BR}} (B \rightarrow D^* \tau^+ \nu)^{[8.5, 9.0]}$	0.09592	0.2σ	0.2σ
483	$\langle \text{BR} \rangle (D^0 \rightarrow \pi^- e^+ \nu_e)^{[0.6, 0.9]}$	0.00042659	0.2σ	0.2σ
484	$\mu_{Vh}(h \rightarrow \gamma\gamma)$	1	0.2σ	0.2σ
485	$\langle \frac{dR}{d\theta} \rangle (e^+ e^- \rightarrow W^+ W^-)^{[189.09, 0.2, 0.4]}$	2.187	0.2σ	0.2σ
486	$\text{BR}(B^- \rightarrow K^- \tau^+ e^-)$	0	0.2σ	0.2σ
487	$\langle P_1 \rangle (B^+ \rightarrow K^{*+} \mu^+ \mu^-)^{[15, 19]}$	-0.62305	0.2σ	0.2σ
488	$\text{BR}(K^+ \rightarrow \mu^+ \nu)$	0.63363	0.2σ	0.2σ
489	$\text{BR}(D_s \rightarrow \mu^+ \nu_\mu)$	0.0054607	0.2σ	0.2σ
490	$\langle \frac{dR}{d\theta} \rangle (e^+ e^- \rightarrow W^+ W^-)^{[205.92, 0.6, 0.8]}$	4.445	0.19σ	0.19σ
491	$\langle A_T^{\text{Im}} \rangle (B^0 \rightarrow K^{*0} e^+ e^-)^{[0.000784, 0.257]}$	0.00024911	0.19σ	0.19σ
492	$\text{BR}(B^- \rightarrow \pi^- \tau^+ \mu^-)$	0	0.18σ	0.18σ
493	$\langle \text{BR} \rangle (D^+ \rightarrow K^0 e^+ \nu_e)^{[0.6, 0.8]}$	0.01225	0.18σ	0.18σ
494	$\langle \text{BR} \rangle (D^0 \rightarrow \pi^- e^+ \nu_e)^{[0.2, 0.4]}$	0.00032822	0.18σ	0.18σ
495	$\text{BR}(\tau^+ \rightarrow \pi^+ \bar{\nu})$	0.1084	0.14σ	0.18σ
496	$\langle P'_6 \rangle (B^+ \rightarrow K^{*+} \mu^+ \mu^-)^{[4, 6]}$	-0.031578	0.16σ	0.17σ
497	$\frac{\langle \text{BR} \rangle}{\text{BR}} (B \rightarrow D^* \tau^+ \nu)^{[6.5, 7.0]}$	0.088532	0.17σ	0.17σ
498	$\frac{\langle \text{BR} \rangle}{\text{BR}} (B \rightarrow D \tau^+ \nu)^{[7.0, 7.5]}$	0.089807	0.17σ	0.17σ
499	$\langle P_1 \rangle (B^0 \rightarrow K^{*0} \mu^+ \mu^-)^{[1, 2]}$	0.039964	0.17σ	0.16σ
500	$\text{BR}(B \rightarrow X_s \gamma)$	0.00033088	0.13σ	0.16σ
501	Γ_W	2.0917	0.16σ	0.16σ
502	$\text{BR}(B^0 \rightarrow K^{*0} \gamma)$	4.1779×10^{-5}	0.17σ	0.16σ
503	$\langle \frac{d\text{BR}}{dq^2} \rangle (B^\pm \rightarrow \pi^\pm \mu^+ \mu^-)^{[2, 4]}$	5.9829×10^{-10}	0.16σ	0.16σ
504	$\langle \frac{dR}{d\theta} \rangle (e^+ e^- \rightarrow W^+ W^-)^{[182.66, 0.8, 1.0]}$	5.434	0.15σ	0.15σ
505	$\langle P'_8 \rangle (B^0 \rightarrow K^{*0} \mu^+ \mu^-)^{[15, 19]}$	0.00073815	0.14σ	0.15σ
506	$\langle \text{BR} \rangle (D^0 \rightarrow K^- e^+ \nu_e)^{[0.8, 0.9]}$	0.0020392	0.14σ	0.14σ
507	$\mathcal{F}t(^{62}\text{Ga})$	4.6665×10^{27}	0.14σ	0.14σ
508	$\langle \frac{d\text{BR}}{dq^2} \rangle (B^0 \rightarrow K^{*0} \mu^+ \mu^-)^{[1, 2]}$	4.5137×10^{-8}	0.18σ	0.14σ
509	$\langle R_{\mu e} \rangle (B^\pm \rightarrow K^\pm \ell^+ \ell^-)^{[0.045, 1.1]}$	0.98175	0.14σ	0.14σ
510	$\frac{\langle \text{BR} \rangle}{\text{BR}} (B \rightarrow D^* \tau^+ \nu)^{[5.0, 5.5]}$	0.057217	0.14σ	0.14σ
511	$\langle \text{BR} \rangle (D^0 \rightarrow K^- e^+ \nu_e)^{[0.7, 0.8]}$	0.0022876	0.13σ	0.13σ
512	$\frac{\langle \text{BR} \rangle}{\text{BR}} (B \rightarrow D \tau^+ \nu)^{[8.0, 8.5]}$	0.082027	0.13σ	0.13σ
513	$\sigma_{\text{trident}} / \sigma_{\text{trident}}^{\text{SM}}$	1	0.13σ	0.13σ
514	$\text{BR}(B^+ \rightarrow \mu^+ \nu)$	3.9386×10^{-7}	0.52σ	0.13σ
515	$\langle P'_4 \rangle (B^0 \rightarrow K^{*0} \mu^+ \mu^-)^{[1.1, 2.5]}$	-0.066752	0.09σ	0.13σ
516	$\langle F_L \rangle (B^0 \rightarrow K^{*0} \mu^+ \mu^-)^{[15, 19]}$	0.34001	0.13σ	0.13σ
517	$\frac{\langle \text{BR} \rangle}{\text{BR}} (B \rightarrow D^* \tau^+ \nu)^{[9.33, 9.86]}$	0.087024	0.13σ	0.13σ
518	$\langle P'_6 \rangle (B^+ \rightarrow K^{*+} \mu^+ \mu^-)^{[2.5, 4]}$	-0.046343	0.12σ	0.13σ

	Observable	NP prediction	NP pull	SM pull
519	$R(e^+e^- \rightarrow W^+W^-)^{[201.6]}$	1	0.12σ	0.12σ
520	$\text{BR}(D^0 \rightarrow \pi^-\mu^+\nu_\mu)$	0.0026933	0.12σ	0.12σ
521	$\langle P_1 \rangle(B^+ \rightarrow K^{*+}\mu^+\mu^-)^{[2.5, 4]}$	-0.097321	0.14σ	0.12σ
522	$\text{BR}(D^+ \rightarrow \pi^0\mu^+\nu_\mu)$	0.0034672	0.12σ	0.12σ
523	$\langle \text{BR} \rangle(D^0 \rightarrow K^-e^+\nu_e)^{[0.6, 0.8]}$	0.004826	0.11σ	0.11σ
524	$\langle \bar{S}_4 \rangle(B_s \rightarrow \phi\mu^+\mu^-)^{[4.0, 6.0]}$	-0.21123	0.13σ	0.11σ
525	$\langle P_3 \rangle(B^+ \rightarrow K^{*+}\mu^+\mu^-)^{[1.1, 2.5]}$	0.0030985	0.11σ	0.11σ
526	$\langle \text{BR} \rangle(D^0 \rightarrow K^-e^+\nu_e)^{[0.4, 0.5]}$	0.0030445	0.11σ	0.11σ
527	$\langle \frac{dR}{d\theta} \rangle(e^+e^- \rightarrow W^+W^-)^{[198.38, -0.2, 0.0]}$	1.265	0.1σ	0.1σ
528	$\langle R_{\mu e} \rangle(B^+ \rightarrow K^{*+}\ell^+\ell^-)^{[0.1, 8.0]}$	0.99442	0.1σ	0.1σ
529	$\frac{\langle \text{BR} \rangle}{\text{BR}}(B \rightarrow D\tau^+\nu)^{[5.07, 5.6]}$	0.077138	0.1σ	0.1σ
530	$\frac{\langle \text{BR} \rangle}{\text{BR}}(B \rightarrow D\tau^+\nu)^{[5.6, 6.13]}$	0.087796	0.1σ	0.1σ
531	$\langle \frac{dR}{d\theta} \rangle(e^+e^- \rightarrow W^+W^-)^{[205.92, -0.2, 0.0]}$	1.231	0.097σ	0.097σ
532	$\langle \text{BR} \rangle(D^0 \rightarrow K^-e^+\nu_e)^{[1.0, 1.2]}$	0.0028671	0.094σ	0.094σ
533	A_c	0.66752	0.092σ	0.092σ
534	$\ln(C)(K^+ \rightarrow \pi^0\mu^+\nu)$	0.19988	0.091σ	0.091σ
535	$R_T(K^+ \rightarrow \pi^0\mu^+\nu)$	-0	0.085σ	0.085σ
536	$\langle P'_6 \rangle(B^+ \rightarrow K^{*+}\mu^+\mu^-)^{[0.1, 0.98]}$	-0.049844	0.09σ	0.084σ
537	$\frac{\langle \text{BR} \rangle}{\text{BR}}(B \rightarrow D^*\tau^+\nu)^{[8.0, 8.5]}$	0.098399	0.084σ	0.084σ
538	$\frac{\langle \text{BR} \rangle}{\text{BR}}(B \rightarrow D^*\tau^+\nu)^{[9.0, 9.5]}$	0.089546	0.082σ	0.082σ
539	$\langle D_{P'_4}^{\mu e} \rangle(B^0 \rightarrow K^{*0}\ell^+\ell^-)^{[14.18, 19.0]}$	-8.6525×10^{-6}	0.072σ	0.072σ
540	$\frac{\langle \text{BR} \rangle}{\text{BR}}(B \rightarrow D\tau^+\nu)^{[5.0, 5.5]}$	0.07073	0.066σ	0.066σ
541	$\langle P'_4 \rangle(B^0 \rightarrow K^{*0}\mu^+\mu^-)^{[15, 19]}$	-0.63503	0.065σ	0.063σ
542	$\langle P_2 \rangle(B^0 \rightarrow K^{*0}\mu^+\mu^-)^{[1.1, 2.5]}$	-0.45619	0.1σ	0.055σ
543	$\frac{\langle \text{BR} \rangle}{\text{BR}}(B \rightarrow D^*\tau^+\nu)^{[9.5, 10.0]}$	0.077738	0.053σ	0.053σ
544	$\langle \bar{S}_7 \rangle(B_s \rightarrow \phi\mu^+\mu^-)^{[15.0, 18.9]}$	-0.0011171	0.055σ	0.053σ
545	$\text{BR}(B^+ \rightarrow K^{*+}\gamma)$	4.2457×10^{-5}	0.039σ	0.052σ
546	$\mathcal{F}t(^{42}\text{Sc})$	4.6665×10^{27}	0.053σ	0.049σ
547	$\langle \frac{d\text{BR}}{dq^2} \rangle(B^+ \rightarrow K^{*+}\mu^+\mu^-)^{[2, 4.3]}$	4.4219×10^{-8}	0.17σ	0.044σ
548	R_c^0	0.17222	0.04σ	0.039σ
549	$\frac{\langle \text{BR} \rangle}{\text{BR}}(B \rightarrow D^*\tau^+\nu)^{[4.0, 4.53]}$	0.028567	0.026σ	0.026σ
550	$\langle \text{BR} \rangle(D^0 \rightarrow K^-e^+\nu_e)^{[0.6, 0.7]}$	0.0025383	0.025σ	0.025σ
551	$\mu_{gg}(h \rightarrow \tau^+\tau^-)$	1	0.025σ	0.025σ
552	$\mathcal{F}t(^{34}\text{Cl})$	4.6665×10^{27}	0.025σ	0.021σ
553	$\langle \text{BR} \rangle(D^0 \rightarrow K^-e^+\nu_e)^{[0.8, 1.0]}$	0.003833	0.018σ	0.018σ
554	$\text{BR}(D_s \rightarrow \tau^+\nu_\tau)$	0.053565	0.3σ	0.018σ
555	$\frac{\langle \text{BR} \rangle}{\text{BR}}(B \rightarrow D\tau^+\nu)^{[9.33, 9.86]}$	0.063888	0.016σ	0.016σ
556	$\langle R_{\mu e} \rangle(B^0 \rightarrow K^{*0}\ell^+\ell^-)^{[0.045, 1.1]}$	0.92444	0.026σ	0.015σ
557	$\text{BR}(D^0 \rightarrow K^-e^+\nu_e)$	0.035522	0.013σ	0.013σ
558	$\langle \text{BR} \rangle(D^+ \rightarrow K^0e^+\nu_e)^{[0.8, 1.0]}$	0.009741	0.007σ	0.0069σ
559	$\langle P'_8 \rangle(B^+ \rightarrow K^{*+}\mu^+\mu^-)^{[2.5, 4]}$	-0.015875	0.0052σ	0.0056σ
560	$\langle P'_8 \rangle(B^0 \rightarrow K^{*0}\mu^+\mu^-)^{[0.1, 0.98]}$	-0.0024076	0.023σ	0.0046σ
561	$\text{BR}(B^0 \rightarrow \tau^+\tau^-)$	2.1776×10^{-8}	0.0045σ	0.0044σ
562	$\text{BR}(B^+ \rightarrow e^+\nu)$	9.2199×10^{-12}	$1.5 \times 10^{-5}\sigma$	$1.9 \times 10^{-5}\sigma$
563	$\text{BR}(\bar{B}^0 \rightarrow \bar{K}^{*0}e^+\mu^-)$	0	0σ	0σ
564	$\text{BR}(B^- \rightarrow K^-e^+\mu^-)$	0	0σ	0σ
565	$\text{BR}(B^- \rightarrow K^-\mu^+e^-)$	0	0σ	0σ
566	$\text{BR}(B^- \rightarrow K^-\mu^+\tau^-)$	0	0σ	0σ
567	$\text{BR}(B^- \rightarrow \pi^-\mu^+\tau^-)$	0	0σ	0σ

	Observable	NP prediction	NP pull	SM pull
568	$\text{BR}(\bar{B}^0 \rightarrow e^\pm \mu^\mp)$	0	0σ	0σ
569	$\text{BR}(\bar{B}^0 \rightarrow e^\pm \tau^\mp)$	0	0σ	0σ
570	$\text{BR}(\bar{B}^0 \rightarrow \mu^\pm \tau^\mp)$	0	0σ	0σ
571	$\text{BR}(\bar{B}_s \rightarrow e^\pm \mu^\mp)$	0	0σ	0σ
572	$\text{BR}(\bar{B}_s \rightarrow \mu^\pm \tau^\mp)$	0	0σ	0σ
573	$\text{BR}(\bar{B}^0 \rightarrow \pi^0 e^\pm \mu^\mp)$	0	0σ	0σ
574	$\text{BR}(B^- \rightarrow \pi^- e^\pm \mu^\mp)$	0	0σ	0σ
575	$\text{BR}(K_L \rightarrow e^\pm \mu^\mp)$	0	0σ	0σ
576	$\text{BR}(\mu^- \rightarrow e^- e^+ e^-)$	0	0σ	0σ
577	$\text{BR}(\mu \rightarrow e\gamma)$	0	0σ	0σ
578	$\text{BR}(\tau^- \rightarrow e^- e^+ e^-)$	0	0σ	0σ
579	$\text{BR}(\tau^- \rightarrow \mu^- e^+ e^-)$	0	0σ	0σ
580	$\text{BR}(\tau \rightarrow \mu\gamma)$	0	0σ	0σ
581	$\text{BR}(\tau^- \rightarrow \mu^- \mu^+ \mu^-)$	0	0σ	0σ
582	$\text{BR}(\tau^- \rightarrow e^- \mu^+ \mu^-)$	0	0σ	0σ
583	$\text{BR}(\tau^- \rightarrow \mu^- e^+ \mu^-)$	0	0σ	0σ
584	$\text{BR}(\tau \rightarrow e\gamma)$	0	0σ	0σ
585	$\text{BR}(\tau^+ \rightarrow \rho^0 e^+)$	0	0σ	0σ
586	$\text{BR}(\tau^+ \rightarrow \rho^0 \mu^+)$	0	0σ	0σ
587	$\text{BR}(\tau^+ \rightarrow \phi e^+)$	0	0σ	0σ
588	$\text{BR}(\tau^+ \rightarrow \phi \mu^+)$	0	0σ	0σ
589	$CR(\mu - e)$ in $^{48}_{22}\text{Ti}$	0	0σ	0σ
590	$CR(\mu - e)$ in $^{197}_{79}\text{Au}$	0	0σ	0σ
591	$\text{BR}(Z^0 \rightarrow e^\pm \mu^\mp)$	0	0σ	0σ
592	$\text{BR}(Z^0 \rightarrow e^\pm \tau^\mp)$	0	0σ	0σ
593	$\text{BR}(Z^0 \rightarrow \mu^\pm \tau^\mp)$	0	0σ	0σ